LUND UNIVERSITY

LUND UNIVERSITY

Analysis of bladder cancer treatment plans generated for online adaptive radiotherapy and validation of an integrated independent dose calculation software

Daria Badika

Supervisors:
Lucie Calmels, Patrik Sibolt, Lina Andersson, and David Sjöström

This project was conducted at the Radiotherapy Research Unit, Department of Oncology, Herlev Hospital

Popular scientific summary in Swedish

Det finns olika strålterapitekniker som används för att behandla cancer. Extern strålbehandling är den vanligaste formen av strålterapi. Syftet med extern strålbehandling är att döda eller bromsa cancercellens tillväxt genom att inducera strålskador i DNA, som kommer påverka deras mekanismer och leda till döden. Den effekt uppnås när höga doser levereras till tumören. Problemet som uppstår vid användning av den här metoden är att man inducerar strålskador även i friska celler, som har allmänt en bättre reparationsförmåga och överlever. Bestrålning av friska vävnader har alltid varit ett huvudproblem för cancer i urinblåsan. Blåscancer är bland de hårdaste urologiska sjukdomarna att behandla med strålterapi på grund av kontinuerlig variation i urinblåsan. För att ta hänsyn till plötsliga volymförändringar används stora behandlingsmarginaler för att säkerställa täckning av behandlingsområdet. Förutom detta är blåsan belägen i bäckenområdet där radiokänsliga organ befinner sig. Leverera höga doser till dessa organ kan ge upphov till olika bieffekter.

Men i dagens läge förbättras tekniken kontinuerligt, strålterapi har blivit mer personlig, noggrannare och effektivare. En ny online adaptiva metod för behandling av blåscancer har utvecklats där artificiell intelligens utnyttjas för att anpassa behandling till dagens anatomi. Innan behandlingsstart kommer patienten för datortomografi, bildtagning som behövs för att avgränsa urinblåsan och rita andra organ i riskzonen som riskerar att få för höga doser. Bilder med definierad struktur används för att generera en behandlingsplan. Vid behandlingstillfället sker ytterligare en biltagning. I den bildtagningen kommer artificiell intelligens att rita om tidigare strukturen. Därefter, börjar systemet generera två olika plan. Den enda planen är beräknad med avseende på dagens anatomi. Den andra planen är beräknad och optimerad till dagens anatomi. Planen som är bäst är vald for behandlingen. Det tillvägagångssättet gör det möjligt att minska behandlingsmarginalerna och skona friska vävnader som omger blåsan. Dessutom, den absorberade dosen till organ i riskzonen kan också minimeras.

Innan behandlingen påbörjas måste planen verifieras. Detta görs för att säkerställa att dosfördelningen i tumören stämmer överens med läkarnas ordination. Traditionellt görs verifiering genom att leverera plan till ett fantom som kommer beräkna skillnaden i den planerade dosen och den levererade dosen. Om inga avvikelser upptäcks blir planen godkänd för behandling. Med den nya online adaptiva metoden är det inte möjligt att avbryta redan påbörjat behandlingen och verifiera den nya genererade planen. Därför utförs planverifiering med hjälp av oberoende dosberäkningsprogramvara.

I detta examensarbete utfördes en retrospektiv studie av sex urinblåscancer patienter som behandlades med online adaptiva metod där de två olika generade adaptiva planer (minskade marginaler) jämfördes med varandra och med det konventionella sättet (med stora marginaler). Resultatet visade att behandlingsmarginalerna kan reduceras 33-55 procent och behålla behandlingsvolymens täckning med hänsyn till att planen är beräknad och optimerad till dagens anatomi. Den oberoende dosberäkningsprogram har också validerats med fantommätningar, vilket innebär att det är ett pålitligt verktyg för planverifiering.

Abstract

Purpose: In 2019 Varian Ethos^{TM} linear accelerator (Varian Medical Systems, CA, USA) with integrated artificial intelligence (AI) was installed at Herlev Hospital, Copenhagen, Denmark, enabling online adaptive radiotherapy (oART) e.g for bladder cancer patients with a large margin reduction. The AI utilizes so called influencers for initial delineation of the targets and organs at risks (OAR) using reference planning computed tomography (CT) images as a guide. The system generates two plans for the treatment, of which one is re-calculated (scheduled plan) and the other is re-optimized (adapted plan) on the anatomy of the day. Moreover, this treatment approach makes traditional phantom based quality assurance (QA) unavailable. This project was focused on three aims; the reduction of target volume achieved utilizing oART approach instead of conventional image-guided radiation therapy (IGRT); quality analysis of the adapted and scheduled plans; validation of a a commercial solution for an integrated independent dose calculation.

Materials and Methods: In total 6 bladder cancer patients, treated with oART, were included in the study. Volumetric and dosimetric analysis were performed retrospectively for 102 adapted and scheduled plans in terms of target coverage and absorbed dose to OAR, such as Bowel Bag and Rectum. The results were compared to corresponding conventional IGRT plans with regular margins used in the clinic. Additionally, effect of bladder volume variations on absorbed dose to OAR was investigated. Conformity index (CI) and homogeneity index (HI) were computed and compared for adapted and scheduled plans.

Furthermore, 54 adapted plans were automatically transferred to Mobius Adapt (Varian Medical Systems, CA, USA) for verification. Global gamma indexes were calculated using the following criteria : 3%/3 mm, 3%/2 mm and 2%/2 mm, 10% threshold. Results from Mobius Adapt calculations were compared to measured local gamma indexes 3%/2 mm, 20% threshold with Delta^4+ phantom (Scandidos, Upsalla, Sweden).

Results: oART enabled 13 %- 59 % planning target volume (PTV) reduction compared to the conventional approach for the studied patients. For scheduled plans, the results revealed an impact on absorbed dose to Bowel Bag (R^2> 0.7) for cases with large bladder volume variations (median (Q_2) >155 cm^3, interquartile range (IQR) >60 cm^3) during the course treatment, but not to Rectum (R^2< 0.3). Whereas smaller bladder volume variations (Q_2 < 100cm^3, IQR< 30 cm^3) did not affect the dose received neither to Bowel Bag or Rectum (R^2< 0.4, R^2< 0.2). A statistically significant improvement in homogeneity (p< 0.05, two patients p= 0.81, p= 0.42) and conformity (p< 0.05) was obtained in the adapted plans compared to the scheduled. No significant difference (p= 0.82, others p < 0.001) was observed between Delta^4+ local gamma index 3%/2 mm and Mobius Adapt 3%/3 mm.

Conclusion: Adaptation had significant impact on absorbed dose to OAR for all studied patients enabling target coverage, while reducing the PTV volume . An independent dose calculation with Mobius Adapt has been validated for dose verification during oART, where traditional phantom-based approaches are not available.

Acknowledgments

I would like to start with expressing sincere appreciation to my supervisors, who have contributed to this thesis, without any of them this research would not be possible.

Lucie Calmels thank you for helping me exporting and extracting all patient data that took ages, teaching me how to be patient when nothing wanted to work, for helping me analyzing that data and your detailed feedback.

Patrik Sibolt thank you for staying late at the hospital and helping me to do measurements, clarifying a lot of things and giving valuable feedback.

Lina Andersson thank you for your help throughout this project, especially for your cheering mails.

David Sjöström thank you for your motivation and making me to realize the importance of finding the right method.

There is one more person whom I would like to thank. It is my classmate and friend Sevgi. Thank you for not killing me every time I made you to run to catch a buss or a train. And helping me to make sense of a lot of things, especially during the last couple of weeks of the project.

Contents

List of abbreviations

AI artificial intelligence

CI conformity index

CBCT cone beam computed tomography

CT computed tomography

CTV clinical target volume

DTA distance to agreement

DVH dose volume histogram

EBRT external beam radiotherapy

GTV gross tumor volume

HI homogeneity index

IMRT intensity modulated radiation therapy

IGRT image guided radiotherapy

IOE intelligent optimization engine

ITP inverse treatment planning

MLC multileaf collimator

MR magnetic resonance

OAR organs at risk

oART online adaptive radiotherapy

PSQA patient specific quality assurance

PTV planning target volume

QA quality assurance

RT radiotherapy

TPS treatment planning system

TV treated volume

VMAT volumetric modulated arc therapy

Part I

Introduction

Our bodies are formed out of cells that grow and divide. Sometimes during these processes genetic changes can occur, that may lead to uncontrolled cell division. Cancer is a general term used for many types of diseases that can arise in any part of the body due to these genetic changes. An example is bladder cancer, which according to the *"World Health Organisation"* is the 10th most common cancer type worldwide [1]. The type of treatment used for bladder cancer depends on the tumor's clinical stage, size, the grade of growth and patient's overall condition. Historically, bladder cancer has been the most difficult genitourinary malignancy to manage, while also conserving the patients quality of life [2].

External beam radiotherapy is often used as a part of the treatment and is given in several fractions over a certain time. Today's margins for the treatment are based on statistics obtained from an extensive population and are used to cover rapid changes in bladder volume and shape. This causes side effects and possible further future complications. However, with improving technologies, it is possible to make radiotherapy of bladder cancer more individualized.

Some studies have shown possibilities to decrease the treated volume by 40% compared to conventional methods by introducing an individual library of three plans based on the bladder size [3]. Recently, a commercial system was developed and released with the solution to upgrade radiotherapy into online adaptive radiotherapy (oART) with help of artificial intelligence (AI) integrated in the system. The system modifies the treatment plan based on the anatomy of the day using cone beam CT (CBCT) as a base for online adaptation.

In this study, AI-driven and CBCT-based oART of bladder cancer was investigated, with a focus on the following three aims:

1. to calculate the reduction of the planning target volume, and investigate effects on the surrounding healthy tissues,
2. to analyze quality of plans generated during online adaptive workflow,
3. to validate the integrated software for independent dose calculation of oART plans.

Part II

Background

1 Urinary bladder cancer

Urinary bladder is located in the pelvic area just above and behind the pubic zone. Bladder is a muscular sac that stores urine and controls urination. In men the bladder is situated in front of the rectum, while women have the bladder positioned in front of the uterus. The size of the organ varies throughout the day depending on the volume of urine stored.

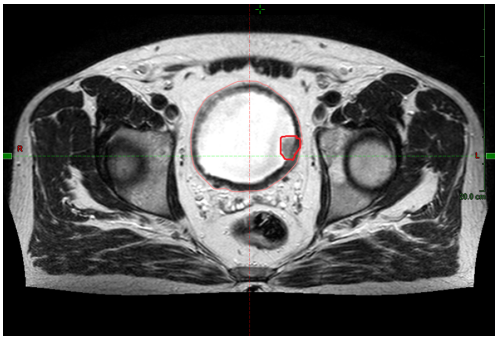

Figure 1: *Transverse magnetic resonance image of a male patient with invasive bladder tumor marked red.*

Worldwide, bladder cancer ranks as the 10th most common malignancy [1]. It can be classified in two stages: non-invasive or muscle-invasive. The main treatment goal for both is to prevent recurrence and progression of the disease. The tumor is surgically removed using cytoscopy, leaving the bladder intact. In some cases different treatment approaches, such as chemotherapy and/or radiotherapy are prescribed.

2 External Beam Radiotherapy of Bladder cancer

Today, external beam radiotherapy (EBRT) is an essential component in cancer treatments due to its survival benefits. Recent advances in technology enable the use of different types of radiation sources like photons, electrons and protons for a better efficacy. The main goal of this method is to use ionizing radiation to induce damage in the tumor cell's DNA.

EBRT uses high energy ionizing particles produced in radiotherapy machines – linear accelerators. Usually bladder cancer patients are treated with photons. The purpose of the treatment is to deliver high doses to the tumor to maximize the tumor control probability and to minimize the normal tissue complication probability [4]. The radiation dose that is delivered to the tumor is measured in Gray (Gy), which is a unit of absorbed radiation that equals to absorbed energy expressed in joule per kilogram of matter 1 Gy= 1 J/kg.

At Herlev Hospital, Copenhagen, Denmark, urinary bladder cancer is treated with a total prescribed dose of 64 Gy. If disease is present in lymph nodes, the area gets a prescribed dose of 50 Gy. The treatment is usually divided into 32 fractions given once a day 5 times a week, which helps to minimize the toxicity to the surrounding tissues. Patients with a low survival expectancy might receive higher doses per fraction over a shorter period.

To deliver an EBRT treatment at Herlev Hospital, patients undergo computer tomography (CT) and magnetic resonance (MR) image acquisition for organ volume delineation. This process is followed by creating personalized treatment plan, which has to be approved and verified.

2.1 Volume Delineation and Margins

The first step in the treatment planning process is delineation and definition of different organs using acquired CT images. There are three main volumes to be considered in radiotherapy planning: gross tumor volume (GTV), clinical target volume (CTV) and planning target volume (PTV) [5] . The volume representing the macroscopic visible position and extent of the malignant growth is GTV, marked red in Figure 2. This volume demonstrates the extent of the tissue with the highest density of the tumor cells.

CTV describes the extent of the possible tumor deposits concealed in the images, shown with pink contours in Figure 2. Usually CTV represents the whole bladder volume with some margins. If there is a lesion in lymph nodes or a known risk of spread, the area will be defined as another CTV and have a different dose prescription than the bladder. To ensure that the CTV receives the prescribed dose, population based margins are added to the structure, leading to an increased morbidity of the healthy tissues surrounding the bladder [6]. This volume is referred to as PTV, which is highlighted blue in Figure 2.

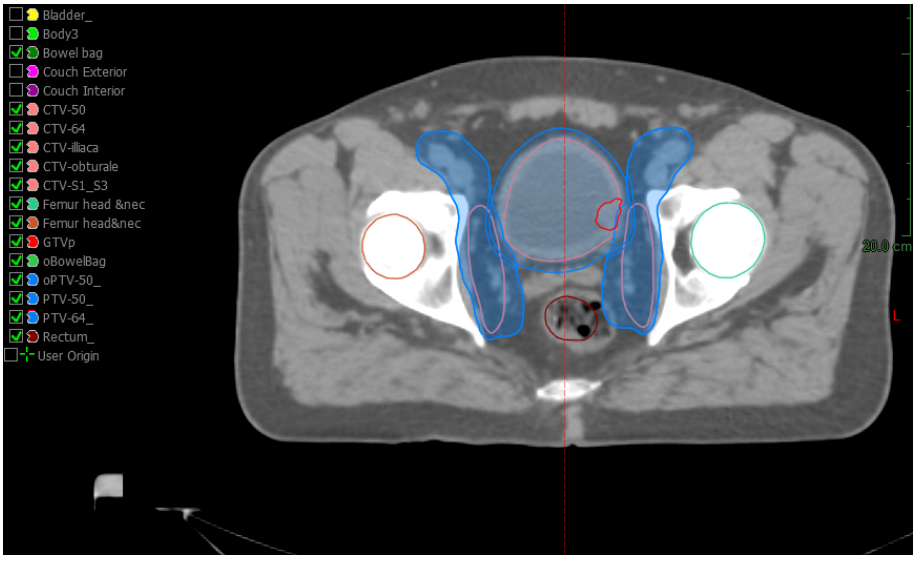

Figure 2: *Transverse CT image slice with delineated GTV, CTV, PTV and organs at risk in a muscle invasive bladder cancer patient including lymph nodes in the treating site.*

Herlev Hospital's conventional bladder protocol applies isotropic 11 mm CTV-PTV margins, except in cranio- caudal direction, where 18 mm is added. These margins help to account for high distensibility of bladder consisting of inter- and intra-fractional variations [7] . The CTV-PTV margins used for oART are smaller compared to the conventional protocol, as oART eliminates inter-fractional motion. At Herlev Hospital, the adaptive

CTV-PTV margins are patient specific. They are calculated based on the inter-fractional variations during the first four treatment fractions.

Organs at risk (OAR) may significantly influence the treatment planning and/or prescribed dose [8]. Normal tissues have distinctive structural organizations divided into parallel and serial subunits. Exceeding tolerance dose level for some of these structures can lead to different side effects. For bladder cancer patients, the OAR are bowel bag, rectum and femoral head. Over irradiation of bowel bag and rectum may cause gastro-intestinal toxicity, which in its turn gives rise to bleeding and faecal incontinence [9, 10]. Risk to develop avascular necrosis is higher when large doses are delivered to the femoral head, making the bones more fragile [11].

2.2 Treatment Planning System and Delivery

Bladder cancer patients are commonly treated with intensity- modulated radiation therapy (IMRT) or volumetric modulated arc therapy (VMAT). The main purpose of IMRT and VMAT is to produce non-uniform absorbed dose distributions by varying intensities and directions within preset beams of a treatment plan. Modulation of the beams is controlled by multileaf collimator (MLC). The main difference between these two approaches is the continuous arc-shaped rotation of the linear accelerator head around the patient during 'beam−on' in VMAT, compared to the static gantry placement in IMRT. The advantage of using these methods is improved dose conformity to the target while minimizing exposure to the surrounding OAR. [12].

IMRT and VMAT treatment planning uses an iterative approach to calculate required intensity for each beam by so called "inverse treatment planning" (ITP). The starting point in ITP is assigning desired dose to clinical constraints with different priorities by user. Dose constraints are converted into objective functions used for optimization of the beam shapes with appropriate intensities, dose rate and gantry rotation to accomplish stated goals. The end result of the treatment planning will be a compromise between the dose delivered to the target and the sparing of OAR. In some cases an OAR structure is adjacent to a CTV-PTV structure creating an overlap. To resolve this problem, a prioritization hierarchy, defined in the stated guidelines, is followed under control of both the physician and medical physicist.

Prescribed radiation dose is delivered in monitor units (MU), calculated by the treatment planning system (TPS). Asymmetrical large targets require a higher number of MU creating more complex plans, resulting in a higher number of treatment fields or arcs [13]. For smaller symmetrical targets generated plans have reduced complexity, with generally lower MU.

In contrast TPS in oART is fully automated requiring minimum manual input. Ethos (described later in section 2.4) TPS utilizes Intelligent Optimization Engine (IOE) algorithm in the optimization process [14]. IOE is used in many steps in oART. For instance in dose preview, interactive dose optimizer allows the user to evaluate effect of potential trade-offs and adjust order of clinical goals if needed before plan generation. During automated planning generation, IOE translates stated clinical goals into objective functions, which helps to control optimization. The system also examines and resolves independently structure

overlap if present. Furthermore, IOE starts optimization process by meeting appropriate requirements for both goal functions and its' stated priority. At the end of the automated planning, IOE suggests a variety of IMRT and VMAT plans for given clinical goals.

2.3 Conventional Workflow

At Herlev Hospital, in a conventional workflow (Figure 3) for bladder cancer patients, target and OARs are delineated using both CT- and MR- images. The plan generated in Eclipse TPS (described in section 2.2) is identical for all fractions scheduled for the patient. If the patients anatomy considerably changes ex. weight loss, alternation in tumor size and etc. a re-planning is needed. For this purpose new CT-images have to be acquired and a new treatment plan has to be created.

Before clinical delivery a generated treatment plans is needed to be approved and verified. This process is called patient specific quality assurance (PSQA) and discussed in more details in section 4.

The positioning of the patient on-couch is facilitated by external markers and knee support. The radiation therapy technologists ensure correct target position every day by acquiring a cone-beam CT (CBCT) at each fraction. If necessary the on-couch correction can be implemented to re-position the target before treatment delivery using automatic soft-tissue match between acquired CBCT and planning CT-images. Thereafter the patient is treated. This treatment approach is called image-guided radiotherapy (IGRT).

Figure 3: *Representation of the conventional workflow at Herlev Hospital. The first step in the process starts with target and OAR delineation. The next two steps are : treatment plan generation in Eclipse TPS (generated plan applied at each fraction), followed by PSQA. Before treatment delivery CBCT is acquired to ensure correct positioning.*

2.4 Online Adaptive Workflow For The Ethos System

The novel approach to oART ,designed to deliver adaptive treatment within 15 minutes, was introduced in 2019, with the launch of Ethos™ therapy (Varian Medical Systems, CA, USA). Ethos is a linear accelerator with a closed bore, equipped with double stacked MLC, with no secondary jaws and field size limited to 28 cm x 28 cm. The machine has a 6 MV flattening filter free beam including pre-configured beam data and a dose rate of up to 800 MU/min (if dose is defined as 1 Gy in d_{max} at a source to surface distance of 100 cm) [14].

The Ethos system is an AI-driven machine with contouring capabilities that is able to use CBCT acquired images for auto-generation of fully re-optimized plans on the anatomy of

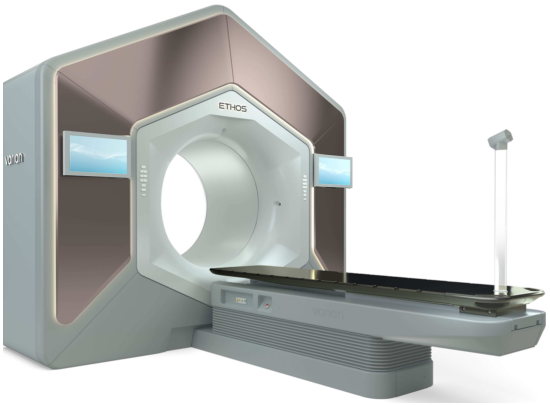

Figure 4: *Ethos linear accelerator with a closed bore design and implemented AI system introduced in 2019 enabling a novel CBCT-based approach to oART [14].*

the day. In Ethos workflow plan generation starts with initial off-couch plan based on the clinical constrains and physician's intent. This plan is then adapted in response to patient's anatomical changes during on-couch generation using CBCT and synthetic CT described further.

2.4.1 Off-couch plan Generation

In adaptive workflow off-couch plan so-called reference plan is generated first in Ethos TPS (Figure 5 marked red).

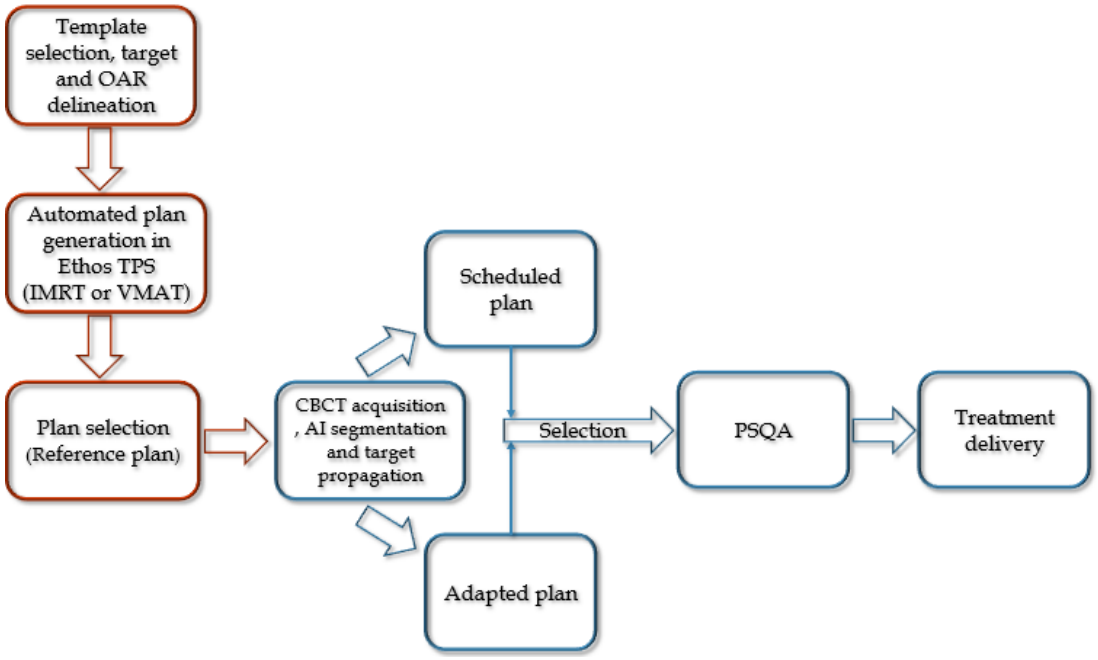

Figure 5: *Representation of online adaptive workflow for the Ethos system at Herlev Hospital. The workflow is divided into two parts: off-couch and on-couch plan generation. Firstly, the system generates off-couch reference plan. After CBCT acquisitions the AI algorithms segment and propagate target and OAR. Based on this anatomy two plans are generated: scheduled and adapted. Selected plan is thereafter verified, approved, and delivered.*

The user starts with selecting the appropriate template from a library of different templates

in the system, with already pre-clinical objectives and dose constraints. The choice of the template depends on the treatment site capturing physician's intentions. CT-images are uploaded into the system for target and OAR contouring followed by generation of the reference plan. The IOE generates a set of 5 plans. These plans that have different beam geometries for the selected template: 7, 9 or 12 fields IMRT, and 2- or 3- arc VMAT. The number of fields and arcs are dependent on the geometrical complexity of the target. IMRT plans generated in Ethos TPS have predefined angles.

Generated IMRT and VMAT plans are later compared to each other with regards to the fulfillment of defined goals and OAR sparing. The reference plan that is the most favorable for the treatment is selected and authorized. This plan serves as the foundation during on-couch adaptation (Figure 5 marked blue).

2.4.2 On-couch plan generation

The second part of adaptive workflow consists of on-couch adaptation, PSQA and treatment delivery (Figure 5 marked blue).

On-couch adaptation starts with patient positioning and CBCT acquisition. As CBCT-image acquisition has been approved, the AI algorithms start segmentation of the organ structures, which influence the shape of the target on the daily CBCT. These structures are called "influences". They have the closest proximity to the target and the biggest impact on the shape of common clinical target structures, and can be edited by the user when needed [14]. For bladder cancer patients the influencers are rectum and bladder predefined by the system as they steer both target- and OAR deformation.

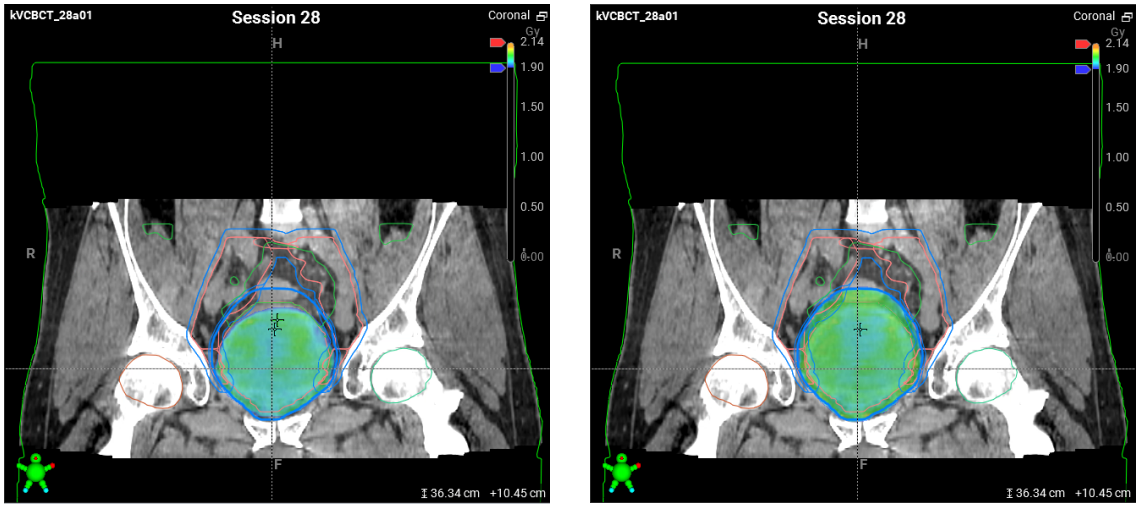

(a) *Re-calculated scheduled plan. A reference plan re-calculated on anatomy of the day leads to partial PTV coverage*

(b) *Re-optimized adapted plan by IOE. A new generated plan adapted on anatomy of the day, with full PTV coverage*

Figure 6: *Dose color-wash on axial CT slice, fraction 28 of a bladder cancer patent treated with oART, demonstrating the PTV high dose coverage for scheduled (6a) and adapted (6b) plan generated on Ethos TPS on-couch.*

As soon as influencer contours are accepted, AI starts to utilize structure guided deformation

algorithm by propagating the CTV structure on the CBCT using planning CT and deriving the PTV from the propagated CTV. As with influencers, the user can manually edit propagated and derived structures if so needed. Once new target and OAR contours have been approved, two plans are automatically generated for review (Figure 6); the scheduled plan (Figure 6a) is the reference plan generated off-couch has re-calculated dose distribution on the anatomy of the day, and the adapted plan (Figure 6b) which is re-optimized by IOE on the anatomy of the day. Dose distribution of the 'new' generated plans is calculated using synthetic CT, which the system generates by deforming the planning CT into daily CBCT.

3 Evaluation of Plan Quality

Dose volume histogram (DVH) is a fundamental tool to determine the optimal plan. It is a simple way to evaluate plan quality by distributing 3D dose values, calculated in TPS, into a graphical 2D format. CT images consist of voxels, containing information about received dose and arranged into different dose bins. By defining a specific dose of desired bin one can extract voxels that receive this dose. This is how a DVH is created.

In addition to DVH metrics, quantities, such as conformity index (CI) and homogeneity index (HI) are used to further evaluate treatment plans. HI characterizes absorbed dose homogeneity distribution within the PTV. While CI characterizes the quality of conformation of absorbed dose within the PTV.

4 Patient Specific Quality Assurance

PSQA is an important part of EBRT. The main purpose of a quality assurance (QA) program is to reduce the likelihood of systematic errors and ensure the accuracy of the delivered absorbed dose. It aims to reveal errors in machine performance, plan selection, by comparing the difference between the planned and delivered dose distributions.

Traditionally, PSQA workflow relies on phantom-based measurements of treatment plan delivery. To verify the treatment plan, using this approach, and avoid possible errors, the plan has to be re-calculated on an artificial data set of a phantom, instead of the actual CT scan [15]. This re-calculated, so called QA plan, is delivered to a phantom. Gamma evaluation is the most commonly used analysis technique and unites percentile dose difference and distance to agreement (DTA) into one metric [16, 17]. The gamma analysis is commonly applied to a given range of the dose distribution, excluding points below a certain dose threshold.

Moreover, there are two different gamma method calculations, that are called global and local. The global gamma usually normalizes the percentile dose difference for each point to the maximum planned dose [18]. The local gamma utilizes a similar technique, except that it uses expected dose at each point instead of maximum planned dose. Thus, gamma indexes obtained for global gamma will always be higher than for local, which was observed by

Ozturk N. et al [19]. The most widely used gamma criteria is 3%/3 mm with 10% threshold as recommended by TG-119 [20, 21, 22].

However, the conventional phantom-based verification method of QA plans is time consuming as it requires phantom positioning and delivery of the QA plan. Some studies have also shown that measured gamma passing rate is dependent on the total number of MU required to deliver the prescribed dose, which is also one of the other parameters defining plan complexity mentioned in section 2.2 [23, 24] . In oART there is no possibility to interrupt the treatment session to perform plan verification. After patients position has been validated with CBCT acquisition, the treatment has to be delivered directly to minimize intra-fractional variations. Online adaptation with the Ethos system uses a commercial software, Mobius Adapt (Varian Medical Systems, CA, USA), for automatic secondary independent dose calculation. Absorbed dose is calculated utilizing the patient's CT-data set and are compared to the planned dose calculated in Ethos TPS. The evaluation of the plan is similar to the conventional phantom measurements, where gamma index is obtained. Calculations are performed using CT delineated structures, which enables comparison of dose differences between target and OAR.

Part III

Materials and Methods

5 Volumetric and Dosimetric Analysis

All plans generated for bladder cancer patients treated with both conventional treatment margins and oART were based on clinical constraints used at the Division of Radiotherapy in the Department of Oncology at Herlev Hospital. The dose constraints are presented in Table 1.

Table 1: *Dose constraints with relative priority for treatment planning of bladder cancer patients at Herlev's hospital, Copenhagen, Denmark.*

Priority	Structure	Constraints
1	PTV-64 Gy	$D_{max} \leq 107\ \%$ $D_{99\%} \geq 60.8$ Gy
1	PTV-50 Gy	$D_{99\%} \geq 47.5$ Gy
2	Rectum	$V_{50Gy} \leq 25\ \%$ $V_{40Gy} \leq 50\%$
2	Bowel Bag	$V_{45Gy} \leq 300\ \text{cm}^3$ $V_{30Gy} \leq 600\ \text{cm}^3$
2	FemoralHead	$D_{max} < 52$ Gy

In total, the study includes 102 sessions for 6 patients. Gender, treatment site and number of adaptive sessions are presented in Table 2. Conventional IGRT plans with regular margins (see section 2.1) were generated at the beginning of the treatment for all patients. The target and OAR were delineated manually by the oncologist for both IGRT and off-couch reference plans. For the on-couch adaptation, the delineation was driven by the AI in the Ethos TPS system and corrected manually by the users online. All the adaptive sessions were exported from Ethos TPS and imported into Eclipse TPS. Each session included: scheduled and adapted plans, adapted structure set and dose distribution calculated with Acuros-XB®. $PTV_{64\ Gy}$ was extracted for all adapted plans and the volume reduction compared to the IGRT approach was calculated.

Data for volume of the target, receiving at least 95 % of the prescribed dose, was extracted for all plans using Eclipse scripting: for obowel bag (bowel bag excluding rectum and bladder) the volume receiving $V_{45\ Gy}$ and $V_{30\ Gy}$ and for rectum the volume receiving $V_{50\ Gy}$ and $V_{40\ Gy}$. Achieved absorbed dose values were compared between the IGRT, reference, scheduled and adapted plans. Correlation between bladder volume variations and absorbed

dose to OAR for adaptive sessions was investigated as well.

Table 2: *Patients included in the study, corresponding gender, treating site and number of adaptive sessions.*

Patient	Gender	Target	# adaptive sessions
1	M	Bladder + lymph nodes+prostate	25
2	F	Bladder	16
3	M	Bladder + lymph nodes	25
4	M	Bladder + lymph nodes+prostate	8
5	F	Bladder	6
6	M	Bladder (hernia)	29

The CI index was calculated according to the *International Commission on Radiation Units and Measurements 62*, equation 1 [13].

$$CI = \frac{TV}{PTV} \tag{1}$$

TV is the volume covered by the $V_{95\,\%}$ isodose [13]. Ideal CI equals to 1, indicating high achieved conformity in the target, whereas lower values indicate partial target coverage. Values greater than 1, demonstrate larger irradiated volume than PTV volume [25].

For IMRT treatment plans *International Commission on Radiation Units and Measurements 83* recommends to use equation 2 to calculate HI [26].

$$HI = \frac{D_{2\%} - D_{98\%}}{D_{50\%}} \tag{2}$$

Where $D_{2\,\%}$ represents the maximum absorbed dose by 2 % of the target volume, $D_{98\,\%}$ is the minimum absorbed dose by 98% of target volume and $D_{50\,\%}$ is the median absorbed dose by 50 % of the volume. Ideal homogeneity in the target is achieved when the HI value is equal to 0. Higher HI values show the opposite i.e an heterogeneous distribution in the target.

Calculated CI and HI values for all studied plans were compared. Statistical analysis was performed between adapted and scheduled plans values.

6 PSQA measurements

At Herlev Hospital, all treatment plans including plans generated during adaptive sessions are verified with Mobius Adapt software. To validate this approach, in total 74 adaptive IMRT plans (Table 3) were re-generated for conventional QA plan delivery to the Delta^4+ phantom (Figure 7). The QA device combines a total of 1069 diodes distributed into two

orthogonal planes inside a cylindrical PMMA phantom. A special algorithm for interpolation estimates doses, at points where no detectors are present [27].

54 Delta^4 pre-treatment plans were generated in Eclipse using analytical anisotropic algorithm algorithm to estimate the expected delivered dose on an artificial CT scan of the QA device. These plans were delivered from gantry angles according to the clinical plan set-up (Table 3).

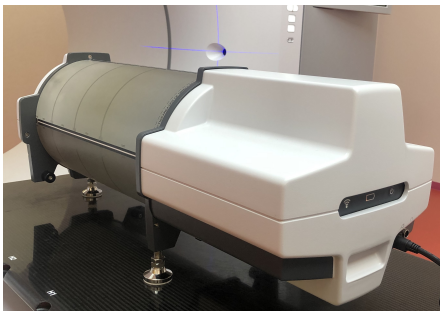

Figure 7: *Representation of Delta^4+ phantom (ScandiDos, Uppsala, Sweden) positioned on the couch for plan delivery*

Re-calculated QA plans were exported to the Delta^4+ software for comparison of the measured dose distribution with the TPS predicted dose distribution using 3%/2mm local gamma, 10 % threshold. In accordance with clinical routine, plans that had a measured local gamma passing rate higher than 90 % were considered to be acceptable.

Furthermore, 20 verification plans were generated with another measuring geometry, where all fields were grouped at 45° gantry angle. The reason for this change is based on the position of the detector plates in Delta^4+ phantom. They can lie parallel to clinical treatment fields causing loss of spatial information, which can give rise to misleading gamma measurements. Plans with 12 fields have 3 fields aligned with Delta ^{4}+ detector boards at 0°, 90° and 270 °. Plans that have 9 fields will have only one gantry angle aligned with Delta ^{4}+, at 0°, whilst plans consisting of 7 fields have none of the fields that are parallel to Delta ^{4}+ detector plates.

Table 3: *Generated and measured QA plans for 6 studied patients with corresponding target volume from the panning CT and number of fields. Measured QA plan geometry was changed only for two patients: Patient 3 and Patient 6.*

Patient	# QA plans clinical set up	# QA plans 45^0 set up	Target volume [cc]	# of fields
1	7	-	1140	12
2	14	-	172	7
3	14	14	974	12
4	8	-	749	12
5	3	-	286	9
6	6	6	675	7

Mobius Adapt (Figure 8) is a dose computational platform where no beam measurements are required. The software uses collapsed cone convolution algorithm to calculate treatment planning (TP) dose distribution using patient's CT data-set. DICOM RT files from the 74 adapted IMRT plans were measured with Delta^4+ phantom, were exported to Mobius Adapt for independent dose calculation. After dose computation, the system applies 3%/3mm

global gamma evaluation with a 20 % threshold at Herlev Hospital. Measured Delta^4+ values were compared to calculated Mobius Adapt.

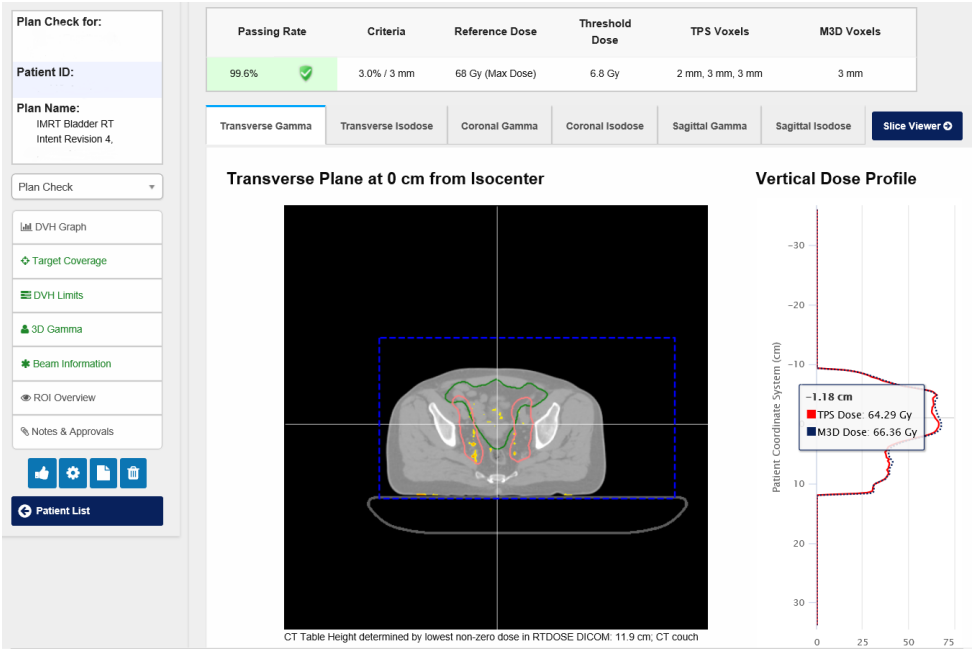

Figure 8: *Representation of Mobius Adapt software. The figure shows transverse synthetic CT slice exported from adaptive session of bladder cancer patient. In the upper right corner patent's information can be found including fraction details. In the lower right corner different features can be viewed, such as DVH, target coverage and beam information. Gamma passing rate together with corresponding criterion showed in the upper middle of the figure. On the figures right one can see vertical dose profile that compares instantly calculated dose in Mobius Adapt to calculated Ethos dose.*

Calculated QA plans were considered to be clinically acceptable if the gamma passing rate was higher than 95 %. Furthermore, additional gamma evaluations were conducted with the following criteria 3%/2mm and 2%/2mm to evaluate sensitivity correlations between measurement- and calculation-based QA.

7 Statistical Analysis

IBM SPSS Statistics software for Mac, Version 26.0 was used for statistical analysis of data. Obtained CI and HI values for adapted and scheduled plans did not follow normal distribution, meaning it was not possible to run a parametric test. The same was applied for measured and calculated gamma indexes. Since data samples are paired but are not normally distributed the Wilcoxon signed rank test was applied. The significance level was set to 0.05 and the null hypothesis assumed that there was no significant difference between investigated values [28].

Part IV

Results

8 PTV Volume Reduction

The PTV volume for the IGRT and adaptive sessions, second quartile (Q_2) which is a PTV median value (more details in section 9), first (Q_1) and third (Q_3) quartiles, interquartile range (IQR) as well as calculated PTV reduction achieved with adaptation, can be observed in Table 4. Patient 3 had the largest PTV volume reduced, while Patient 6 had the lowest.

Table 4: *Extracted PTV volumes of the conventional IGRT plans, calculated Q_2 , Q_1, Q_3, IQR for adaptive sessions including PTV volume reduction compared to the IGRT plan.*

	IGRT PTV [cc]	Adaptive PTV_{Q_2} [cc]	Adaptive PTV_{Q1} [cc]	Adaptive PTV_{Q3} [cc]	Adaptive PTV_{IQR} [cc]	Adaptive Reduction [%]
Patient 1	708.9	438.8	459.2	545.5	86.3	38
Patient 2	312.4	173.4	161.9	179.1	17.2	44
Patient 3	678.3	279.5	255.6	339.7	84.0	59
Patient 4	457.2	297.3	283.1	308.9	25.9	35
Patient 5	436.0	293.6	256.7	308.4	51.7	33
Patient 6	756.6	655.9	596.9	724.9	128	13

9 Volumetric and Dosimetric Results

In this section volumetric and dosimetric results are presented. Monitored bladder volume variations shown in Figure 9), PTV coverage in Figure 10, absorbed dose in obowel bag in Figure 11b, 11a, and rectum in Figure 12b, 12a. Figures include off-couch reference values obtained from the plan calculated on the planning CT, marked bright green. IGRT values with conventional margins marked dark green. Adaptive sessions consisting of adapted and scheduled values marked blacked respective blue. The distribution of data is presented with box and whisker plots known as five number summary plot. Q_1 is a lower part of the box defining 25^{th} percentile. Q_3 is an upper part of the box defining 75^{th} percentile. The size of the box is defined as IQR. It is a distance between 75^{th}- and 25^{th} percentile. Q_2 is a drawn line (marked pink) inside the box illustrates median as 50^{th} percentile. Whiskers are the two lines extended outside of the box to the largest and smallest value from the data set withing the following interval $[Q_1 - 1.5 \cdot IQR; Q_3 + 1.5 \cdot IQR]$ [29]. All observed values outside of the given interval are considered as outliers (marked red). Tables in Appendix A contain more detailed information of corresponding figures with Q_2, Q_1, Q_3 and IQR.

9.1 CTV variations

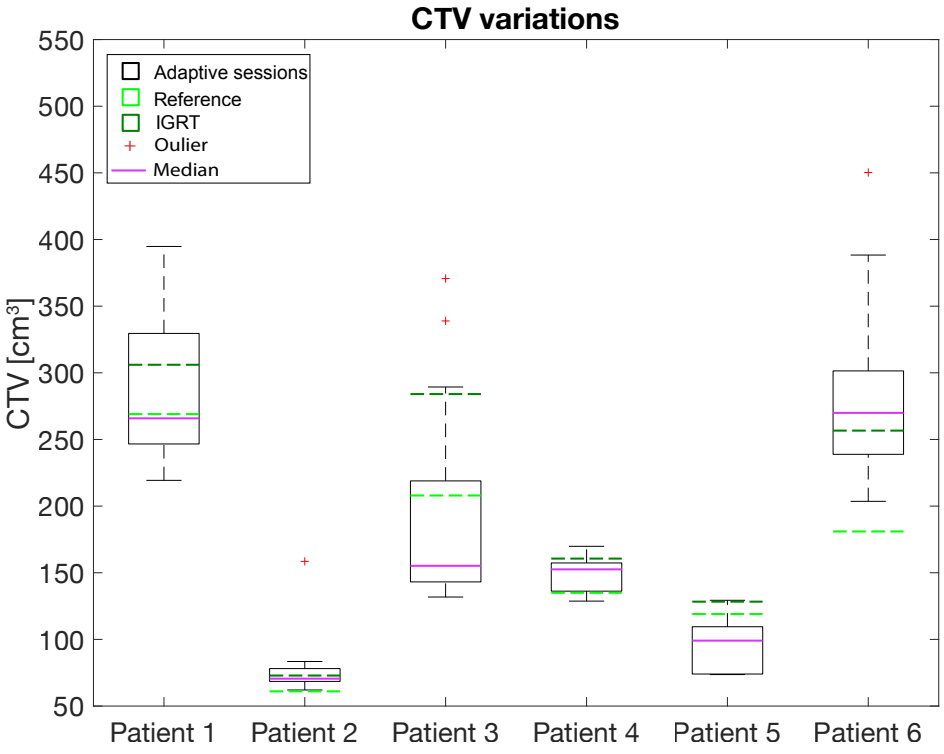

Figure 9: *Variation of CTV volume for off- couch reference plans, IGRT plans with conventional margins and on- couch generated scheduled and adapted plans with corresponding median and outliers.*

Figure 9 shows bladder volume variations along the treatment duration as well as values of corresponding IGRT and off-couch reference plan. Patient 1,3,4 and 6 have larger bladder variations (Q_2> 155 cm^3, IQR> 60 cm^3, Appendix A Table 8) in comparison to Patient 2 and 5 (Q_2< 100 cm^3, IQR < 30 cm^3, Appendix A Table 8) (Figure 9). Delineated CTV volumes on IGRT plan (dark green line) are positioned above the off- couch reference CTV volume (bright green light).

9.2 PTV coverage

Figure 10 displays PTV coverage distribution for oART and IGRT plans. The off-couch reference, on-couch adaptive and IGRT plans present a good target coverage within Herlev's clinical dose constraints (> 99 % of the prescribed dose). On the contrary, the scheduled plans for all patients and all fractions do not fulfill the clinical constraints (< 99 %), with a very poor target coverage for Patient 1 and 6.

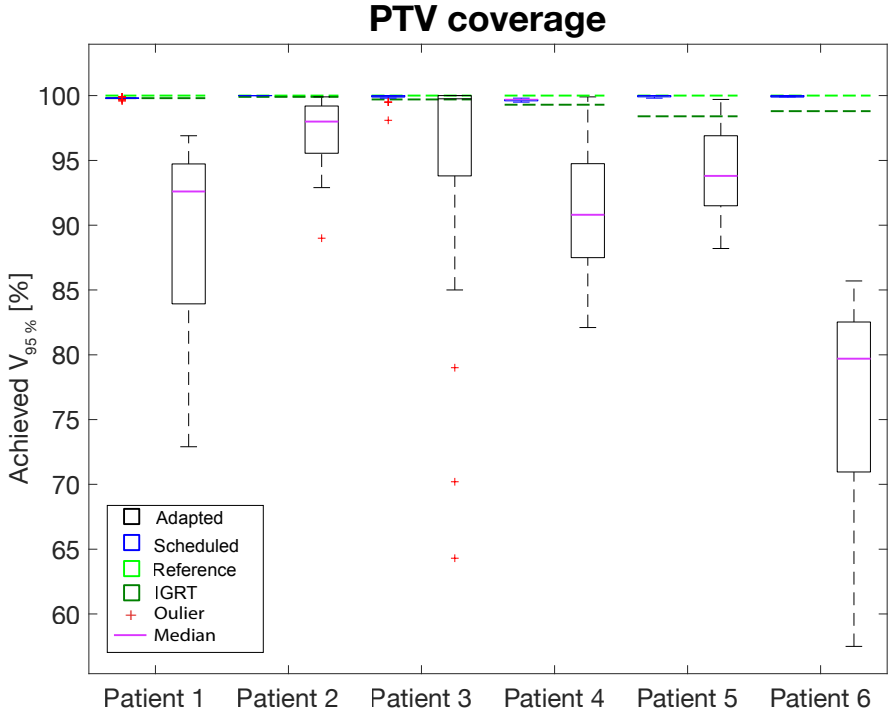

Figure 10: *Achieved PTV coverage for off- couch reference plans, IGRT plans with conventional margins and on-couch generated scheduled and adapted plans with corresponding median and outliers.*

9.3 oBowel Bag $V_{45\,Gy}$ and $V_{30\,Gy}$

Volume of obowel bag receiving $V_{45\,Gy}$ and $V_{30\,Gy}$ is illustrated in figure 11. The dose delivered to the obowel bag is higher for the IGRT plans compared to all the other plans. The median obowel bag $V_{45\,Gy}$ and $V_{30\,Gy}$ values for on-couch adapted plans are closer to the off-couch reference plan values for Patient 1, 2 and 3. For the Patient 4 and 6, the online

adaptive values are higher than the reference values. For Patient 5, the adaptive values are lower than the reference value. The scheduled plans have similar or lower $V_{45\,Gy}$ and $V_{30\,Gy}$ compared to the reference value.

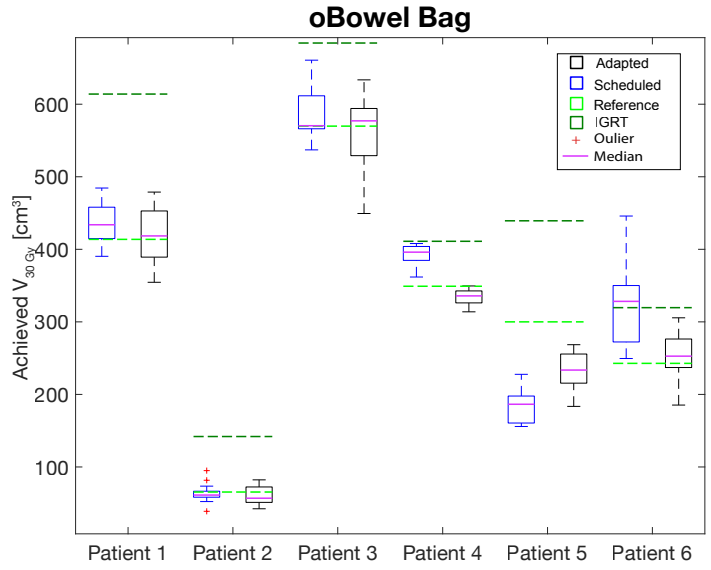

(a) $V_{30\,Gy}$ *achieved volume in oBowel Bag.*

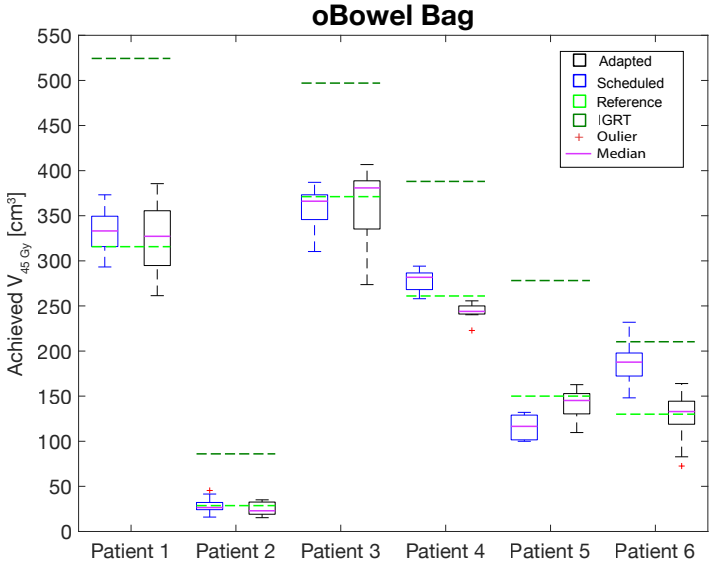

(b) $V_{45\,Gy}$ *achieved volume in oBowel Bag.*

Figure 11: *Achieved volume* $V_{30\,Gy}$ *(11a) and* $V_{45\,Gy}$ *(11b) in obowel bag for off- couch reference plan, corresponding conventional IGRT plan and on- couch generated scheduled and adapted plans with corresponding median and outliers.*

9.4 Rectum $V_{50\,Gy}$ and $V_{40\,Gy}$

Obtained results for rectum $V_{50\,Gy}$ and $V_{40\,Gy}$ are provided in Figure 12. $V_{50\,Gy}$ and $V_{40\,Gy}$ off-couch reference plan values are lower than the IGRT values for all patients, except Patient 5- $V_{40\,Gy}$ (Figure 12a). The adapted median values for $V_{50\,Gy}$ are similar or lower than the reference plan median values for all studied patients, except Patient 1 (Figure 12b).

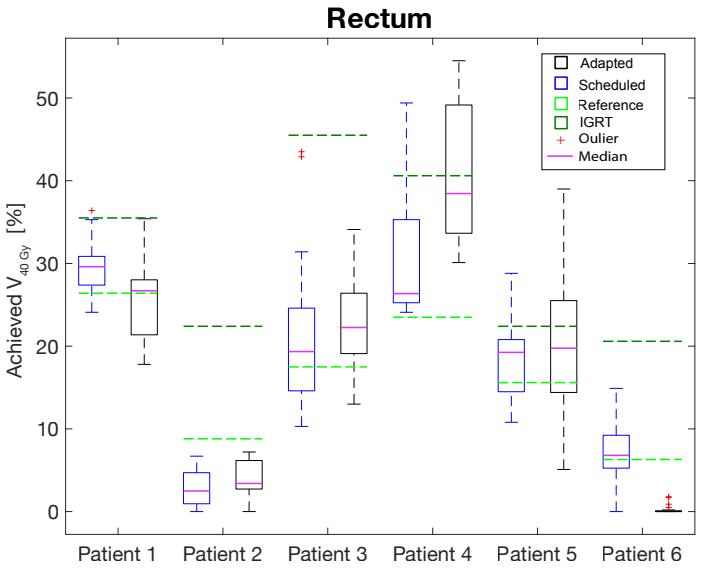

(a) $V_{40\,Gy}$ *achieved volume in rectum.*

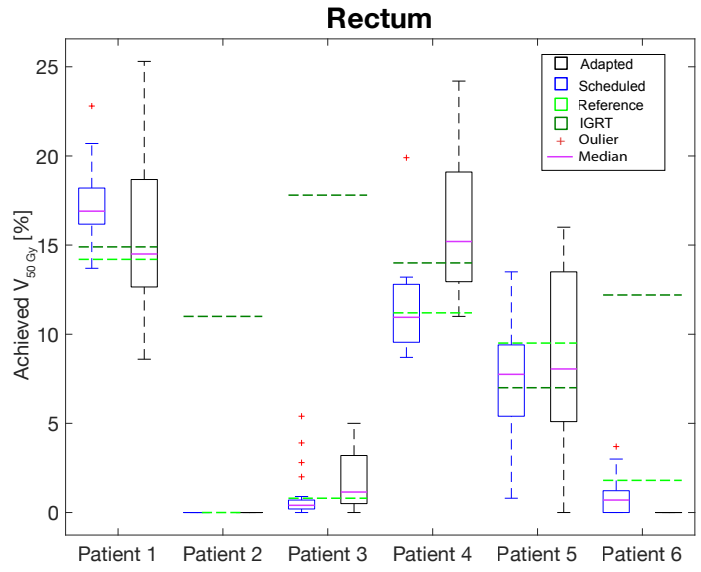

(b) $V_{50\,Gy}$ *achieved volume in rectum.*

Figure 12: *Achieved volume* $V_{40\,Gy}$ *(11a) and* $V_{50\,Gy}$ *(11b) in rectum for off- couch reference plan, corresponding conventional IGRT plan and on- couch generated scheduled and adapted plans with corresponding median and outliers*

The scheduled plans have similar medium values as adapted plans, but with a larger spread

of data (see Q_1 and Q_3 in Appendix A, Table 12). For $V_{40\,Gy}$ the adaptive sessions can not achieved a better sparing of rectum than the reference plans for all patients, except Patient 2 (Figure 12a).

10 Correlation Results

Figure 13 has collection of scatter plots belonging to Patient 2 and Patient 3. Remaining 4 patients are presented in Appendix B. In these plots, correlation coefficient was determined for obowel bag and rectum as a function of bladder volume variation.

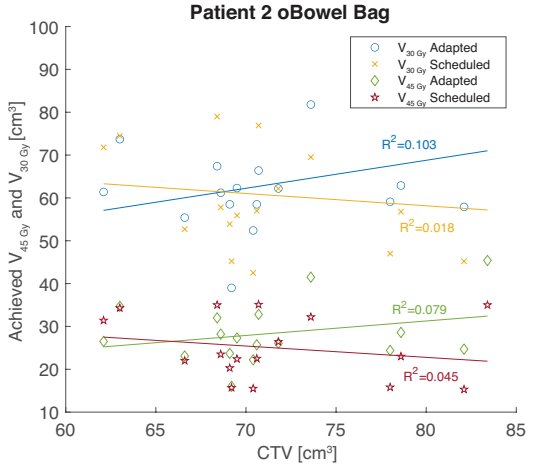

(a) *Variations of obowel bag volume receiving 45 Gy and 30 Gy as a function of bladder volume changes in Patient 2.*

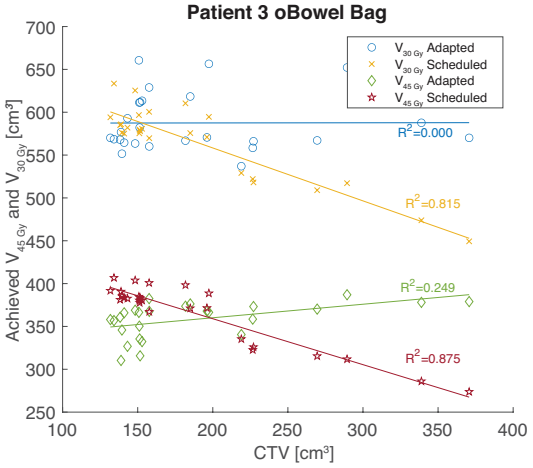

(b) *Variations of obowel bag volume receiving 45 Gy and 30 Gy as a function of bladder volume changes in Patient 3.*

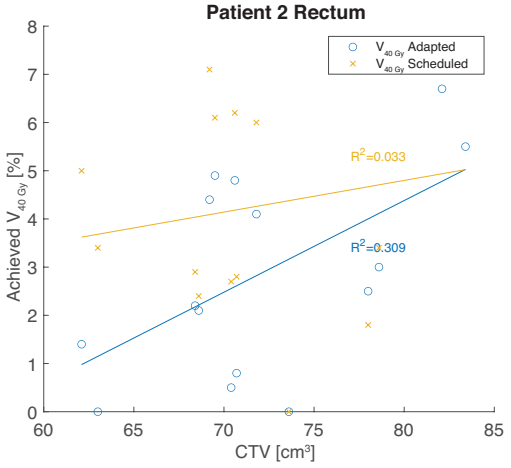

(c) *Variations of rectum volume receiving 50 Gy and 40 Gy as a function of bladder volume changes in Patient 2.*

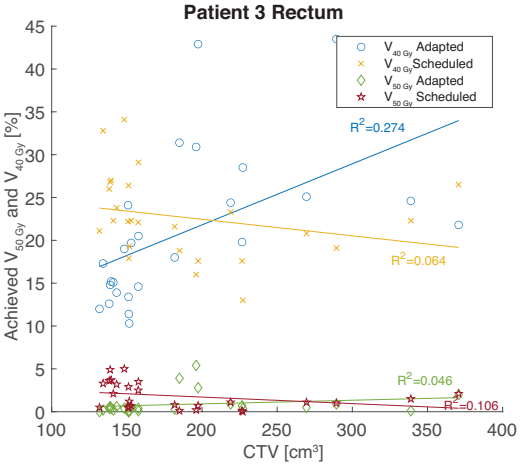

(d) *Variations of rectum volume receiving 50 Gy and 40 Gy as a function of bladder volume changes in Patient 2.*

Figure 13: *Variations of absorbed dose in different OAR as a function of bladder volume changes, in Patient 2 and Patient 3.*

According to the Figure 13c and Figure 13d, there is no correlation between bladder volume variations and absorbed dose to rectum, for both adapted and scheduled plans for all patients (Appendix B). Patient 2 (Figure 13a) and Patients 4, 5, 6 (Appendix B) showed the same tendency for obowel bag, for both scheduled and adapted plans. In contrast Patient 1 (Appendix B) and Patient 3 (Figure 13b) demonstrated decreased dose to obowel bag with increased bladder volume for scheduled plans. This was not observed in adapted plans.

11 Conformity and Homogeneity Indexes Results

Calculated values for CI and HI for IGRT, off-couch reference plan, on-couch generated scheduled and adapted plans are plotted in Figure 14 and Figure 15 respectively . All IGRT and off-couch reference plans have CI equals 1. Online generated on-couch adapted plans have CI calculated values closer to 1 than the scheduled plans, except Patient 2.

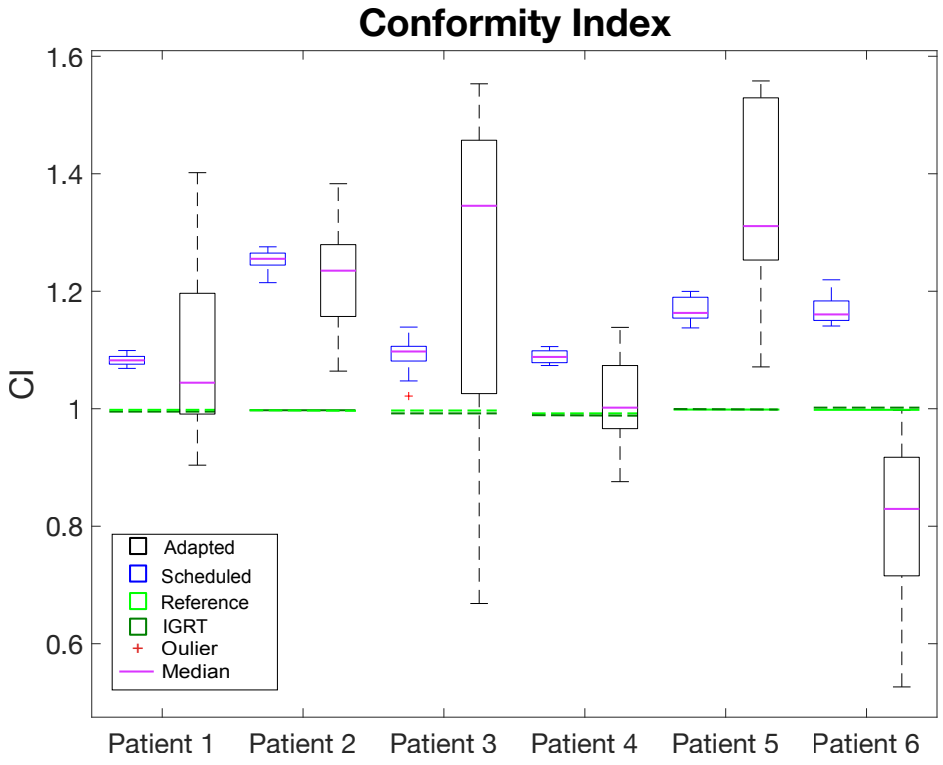

Figure 14: *Calculated CI for off-couch reference plan, corresponding conventional IGRT plan, on-couch generated scheduled and adapted plans.*

There are larger variations of the data for scheduled plans, taking into account that some of the obtain CI median values for Patient 1, 3 and 6 are lower than 1. Patient 6 have all calculated CI values for scheduled plans lower than off-couch reference.

In Figure 15 determined HI for off-couch reference plans are lower than or equal to IGRT plans, except for Patient 4. HI values for adapted plans are closer to both IGRT and off-couch reference plan, compared to scheduled plans. Less spread of the data is noticed in adaptive data relative to scheduled data.

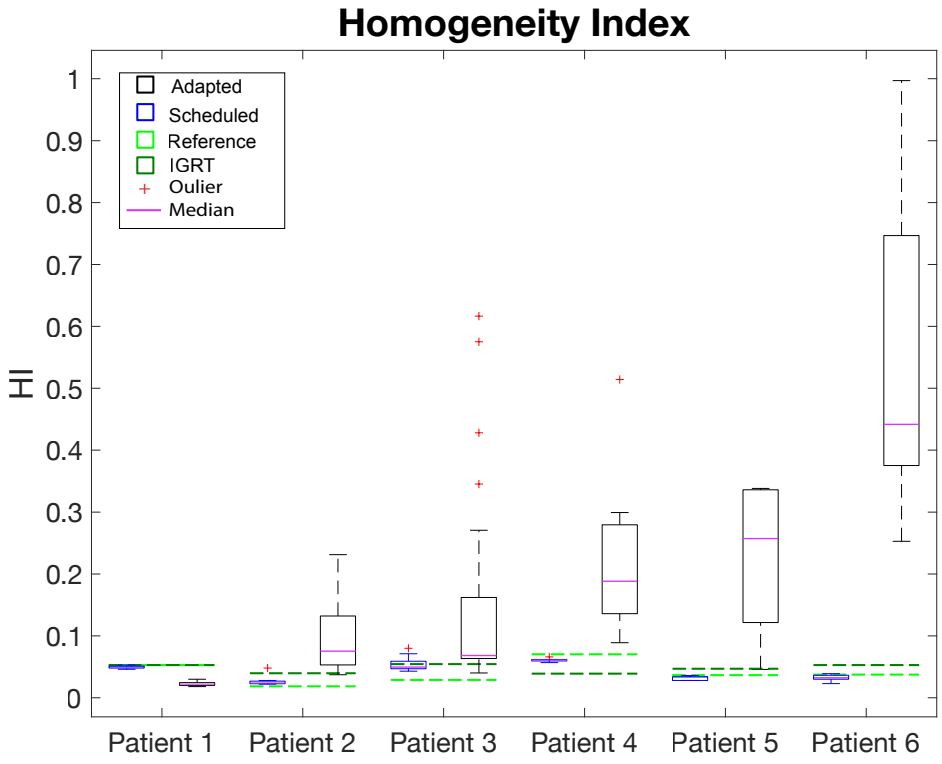

Figure 15: *Calculated HI for off-couch reference plan, corresponding conventional IGRT plan, on-couch generated scheduled and adapted plans.*

Paired Wilcoxon signed rank test was performed to determine if there was a statistical significant difference between calculated adaptive and scheduled CI and HI (Table 5).

Table 5: *Paired Wilcoxon signed rank test of calculated CI and HI values performed between adapted and scheduled plans.*

	n	p_{CI}	p_{HI}
Patient 1	25	0.81	<0.001
Patient 2	17	0.42	<0.001
Patient 3	26	0.008	<0.001
Patient 4	8	0.021	0.008
Patient 5	6	0.028	0.018
Patient 6	30	<0.001	<0.001

As it can be seen in Table 5 there is significant difference between adapted and schedule HI values. The same is valid for CI values, except Patient 1 and Patient 2.

12 PSQA results

Figure 16 represents gamma passing rate for 54 measured with Delta^4 phantom online adapted plans as a function of MU/Gy. There is an indication of decrease in gamma passing rate with increasing MU/Gy.

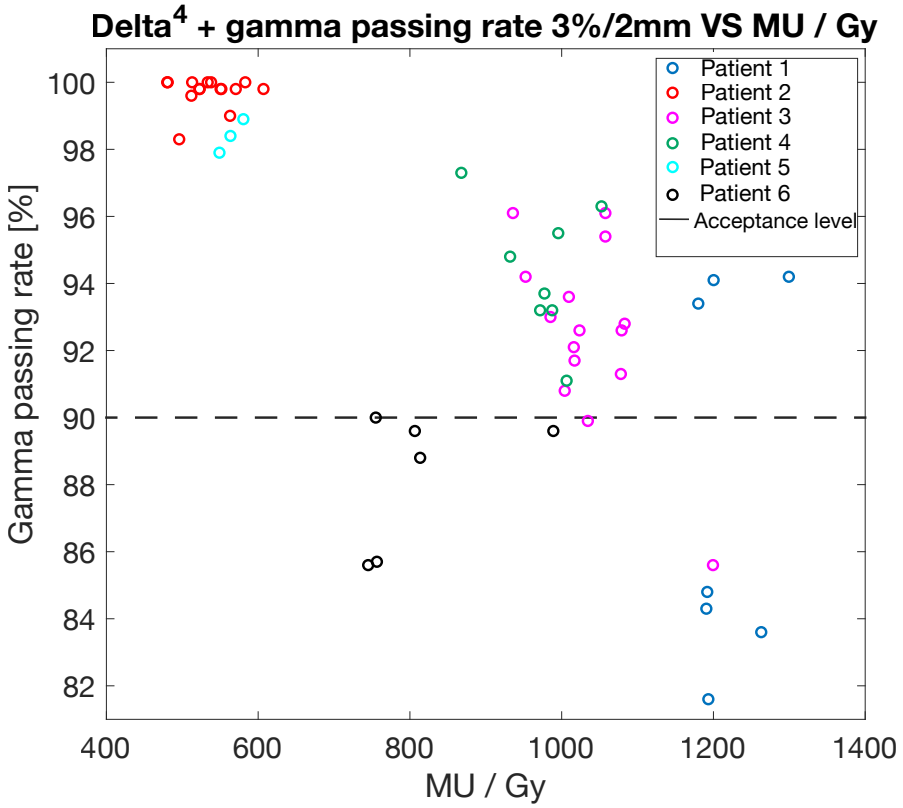

Figure 16: *Delta^4 gamma passing rate measured with 3%/2mm criteria for 54 measured adapted plans. Plans with gamma passing rate higher than acceptance level at 90 % considered to be verified.*

Figure 17 illustrates distribution of gamma index for 74 studied plans. The figure demonstrates measured local gamma passing rate with Delta^4+ phantom 3%/2 mm, threshold 20 % , and calculated global gamma passing rate with Mobius Adapt plans, where different criteria were applied: 3%/3 mm, 3%/2 mm, 2%/2 mm, threshold 10%.

According to the Figure 17 all measured QA plans with Delta^4 had lower gamma passing rates, than calculated Mobius Adapt for all criteria, excluding Patient 2. Higher Delta^4 gamma passing rates were achieved for Patient 3 and Patient 4 at measured gantry angle of 45°. Mobius Adapt calculated gamma gave the highest gamma passing rate for 3%/3 mm criteria , the lowest for 2%/2 mm and 3%/2 mm in between.

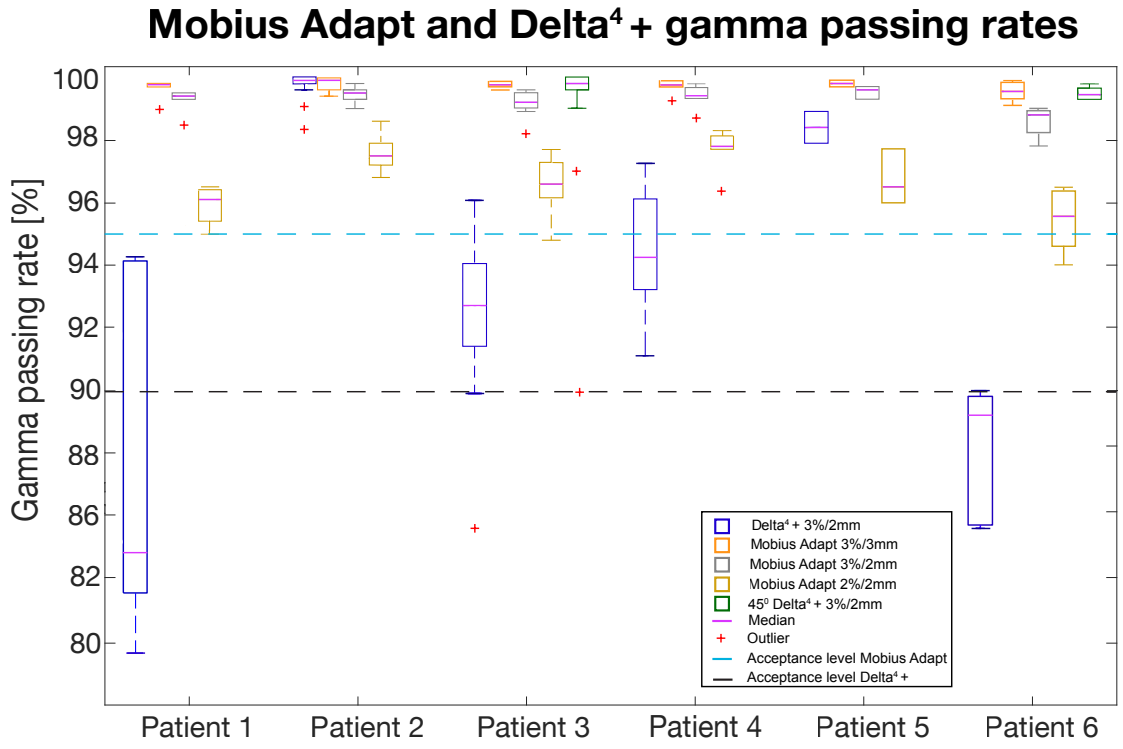

Figure 17: *Gamma passing rate variations for Delta^4+ phantom 3%/2 mm and Mobius Adapt software 3%/2 mm, 2%/2 mm. Measured Delta^4+ and calculated Mobius Adapt plans with gamma passing rate higher that 90% and 90% respectively considered to be verified.*

Paired Wilcoxon ranked test was used to investigate the difference between Delta^4+ measured gamma passing rates and calculated Mobius Adapt (Table 6).

Table 6: *Paired Wilcoxon ranked test between measured local gamma with Delta^4+ phantom 3%/2 mm and calculated global gamma with Mobius Adapt for for 3%/3 mm, 3%/2 mm, 2%/2 mm.*

		p		
	n	Mobius 3D 3%/3 mm	Mobius 3D 3%/2 mm	Mobius 3D 2%/2 mm
Patient 1	7	0.018	0.018	0.018
Patient 2	14	0.513	0.023	0.001
Patient 3	14	0.001	0.001	0.001
Patient 4	8	0.008	0.008	0.008
Patient 5	3	0.066	0.066	0.109
Patient 6	6	0.028	0.028	0.028

There is a significant difference between measured Delta^4+ and calculated Mobius Adapt values. Except for Patient 2 for Mobius Adapt 3%/3 mm and Patient 3 (all Mobius Adapt criteria), where no significant difference was observed.

Paired Wilcoxon ranked test was also applied after irradiation of Delta^4+ at 45° gantry angle and calculated Mobius Adapt. Tables 7 displays no significant difference between 45° Delta^4+ measurements and Mobius Adapt 3%/3 mm, whether there is a significant difference between other criteria.

Table 7: *Paired Wilcoxon ranked test for measured local gamma with Delta^4+ at 45° gantry angle 3%/2 mm and calculated global gamma with Mobius Adapt for for 3%/3 mm, 3%/2 mm, 2%/2 mm .*

		p		
	n	Mobius 3D 3%/3 mm	Mobius 3D 3%/2 mm	Mobius 3D 2%/2 mm
Patient 3	14	0.937	0.012	0.001
Patient 6	6	0.750	0.028	0.028

Part V

Discussion

13 Volumetric and Dosimetric Discussion

In this study a retrospective analysis of plan quality was performed for the 6 patients treated with a novel oART approach, using implemented AI system and CBCT to generate plan of the day. This technique decreases CTV-PTV margins compared to the non-adapted conventional IGRT CTV-PTV margins, as inter-fractional variations are eliminated. Moreover, anatomical changes of the treated patient are monitored, making it possible to adapt the treatment plan according to these changes.

For the 6 patients studied the results showed that PTV volume was reduced by 13%-59% using oART relative to corresponding non-adapted conventional IGRT plans (Table 4). Patient specific margins in oART are calculated based on the four first fractions of bladder inter-fractional variations. As a consequence of CTV-PTV margin reduction, the majority of the scheduled plans had PTV coverage lower than 95 % (Table 10). Patient 6 had hernia, which caused very unusual bladder variations, therefore smaller margin reduction was obtained for this patient, only 13 %.

Furthermore, daily plan generation based on anatomy of the day, allows determination of the actual delivered dose to the target and OAR. Obtained results for bladder variations have confirmed that bladder filling can change drastically from day to day. For conventional radiotherapy of bladder cancer, the margins are population based, accounting for intra- and inter-fractional bladder variations, while enlarging the treated area and delivering higher absorbed dose to radiosensitive organs, such as obowel bag and rectum [9, 10]. Moreover, obowel bag and rectum are movable organs, their size and position also changes daily. Therefore, DVH from the initially generated plans cannot be trusted, since they are based on a single CT acquisition at a specific point in time [30].

According to the results (Figure 9) the delineated bladder volume for the off-couch reference plan was lower in contrast to corresponding conventional IGRT plan for all patients. This difference is seen because in the conventional workflow, the bladder volume is a combination of the manual delineation by the physician on both MR- and CT-images. In the Ethos online adaptive workflow the manual delineation is done only on the CT-images before generation of the off-couch reference plan. During the oART, delineation is AI driven and can be adjusted manually by users.

Investigating the effect of oART on absorbed dose to OAR showed that the dose was dependent on the treating site and extension of the CTV-PTV. In general, if patient had only bladder defined as CTV-PTV, greater OAR sparing was achieved with oART compared to corresponding conventional IGRT plan. oART was not as effective in dose paring to the OAR for patients with elective area and/or prostate prostate included in the CTV-PTV.

For obowel bag, the absorbed dose was higher if elective area was included in the target

compared to the absence of elective area. This was observed in Patients 1, 3, 4 with lymph nodes embedded into CTV-PTV (Table 11). The larger the treated area, the higher dose to the obowel bag was delivered. Moreover, inter-fractional variations were also greater for Patients 1, 3 and 6 (IQR> 69 cm^3, Appendix A Table 8) compared to other patients (IQR< 29 cm^3, Appendix A Table 8). Patients with stable bladder and without lymph nodes included in the PTV, achieved greater sparing of obowel bag in adaptive treatment. Patient 6 with hernia had very large CTV-PTV extension, which contributed to higher doses to the obowel bag.

Correlation computations of bladder volume and absorbed dose to obowel bag using adaptation, showed an impact for scheduled plans for patients with large inter-fractional variations (Table 13). When bladder volume increased, volume of the obowel bag receiving 45 Gy or 30 Gy decreased. This effect was observed, because scheduled plans were only re-calculated on anatomy of the day. The system applied the off-couch reference plan without re-optimization. Therefore, when bladder volume increased, the obowel bag was moved further away from the initial bladder volume delineation and from the re-calculated dose. Consequently, if the bladder was smaller on the reference CT, but larger on daily anatomy, the obowel bag received a smaller dose. For patients with smaller inter-fractional variations this trend was not observed. Moreover, there was no correlation between bladder volume variations and received dose to obowel bag for adapted plans, because in this case the system did a complete re-optimization of the plan based on daily anatomy.

For $V_{50\,Gy}$ and $V_{40\,Gy}$ rectum dose, the results differed between each other. It was demonstrated that for adaptive sessions, greater rectum dose was spared for $V_{50\,Gy}$ than for $V_{40\,Gy}$ compared to the off-couch reference plan.

It appeared that the absorbed dose to rectum for $V_{50\,Gy}$ was target dependent, as part of the rectum was in the high dose area. For patients that had a larger bladder in general and larger volume variations, the absorbed dose to rectum 50 Gy was higher as rectum was located closer to the CTV-PTV. This was seen in Patient 3 and Patient 6. Moreover, each patient physiology also affected $V_{50\,Gy}$ absorbed dose. Some people have rectum located very close to the bladder, even if the bladder size and variations are small, the $V_{50\,Gy}$ becomes relatively higher than if no rectum was inside the CTV-PTV, which was the case with Patient 5. Patient 1 and Patient 4 had prostate included in the PTV. Prostate is located in front of rectum and below bladder, reaching the middle part of the rectum. Therefore, for these patients a larger part of rectum was inside the CTV-PTV, which contributed to an increased $V_{50\,Gy}$.

Adaptive sessions did not achieve a better rectum sparing than the off-couch reference plan, except for Patient 2 with smallest PTV. For $V_{40\,Gy}$ the dose was more dependent on configuration of the beam angle and plan. If the patient had more complex PTV volume, which generated a more complex plan, the dose to the rectum was higher relative to patients with less complex plans.

Computation of CI demonstrated that adaptive sessions had higher CI calculated values than corresponding IGRT or off-couch reference plans. The possible explanation might be related to AI algorithms that perform dose computation. Unfortunately no details are provided how the algorithms works, but it seems that TV on adapted plans were enlarged compared to off-couch treated volume. Thus all calculated values were greater 1. Scheduled

plans were not re-optimized, which affected TV as it was not adapted to patients inter-fractional variations, hence the calculated values were distributed above and under 1.

The HI values were similar between corresponding IGRT, off-couch and on-couch adapted plans. Scheduled plans were not re-optimized, which affected heterogeneity inside the target.

14 PSQA

Earlier studies have demonstrated a high degree of plan complexity affects the gamma passing rate [24]. As discussed earlier in section 2.2, in IMRT plan complexity is related to several parameters that include the total number of MUs and target size.

Overall, measured Delta^4+ gamma passing rates, with fields arranged as in treatment plan, was lower than calculated Mobius Adapt gamma passing rates. Results in Figure 16 showed a dependency between MUs required to deliver prescribed dose and measured gamma passing rate values. Patient 2 and Patient 3, with lowest number of MU/Gy and smallest CTV-PTV volume (only bladder was treated, Table 2 and Table 3) have obtained highest gamma values in contrast to patients with higher MU/Gy and larger treated volume (Table 2 and Table 3). This is especially noticeable in Patient 1, with largest treated area due to several targets included in the treatment as well as highest number of MU/Gy (Table 3). Quite low gamma passing rate for Patient 6 can be explained by the presence of hernia, that forces the bladder to fall into scrotum, giving rise to a more complex treatment plan generation. Measured gamma passing rate for other patients (Patient 4 and Patient 5) had shown the same tendency as for patient 1. The result was dependent on the MU/Gy and planned target volume. These results corresponds with the previous studies that evaluated relationship between the treatment sites, the total number of MUs and passing rate [23].

When the treatment fields were collapsed to 45° gantry angle, the gamma passing rate became significantly higher. Indicating that previously obtained low values were associated with Delta^4+ geometrical factors. As Delta^4+ detector plates align with treating fields as discussed in section 6, it causes loss of spatial information for correct gamma passing rate estimation. Which explains considerable low gamma for patient 1, 3 and 4 and higher gamma passing rate values for Patient 2 and 5. When the phantom was irradiated at 45° gantry angle, geometrical factors were eliminated, in this case detector plates were not aligned with treating fields. Consequently, the values became considerably higher and agreed with calculated passing rate in Mobius Adapt. Based on this results, it was adequate to approve treatment plans what had low measured gamma passing rate.

Varying gamma criteria in Mobius Adapt had shown that the passing rate decreased with stricter criteria. The lowest calculated gamma passing rate was achieved with 2%/2 mm, highest with 3%/3 mm and 3%/2 mm gave results in between. Paired Wilcoxon ranked test illustrated that there was significant difference between measured and calculated gamma passing rate. With exception for some patients, as their measured and calculated gamma rates were in agreeance. For plans, with treatment fields grouped at gantry angle of 45° similar results were observed. The statistical test showed no significant difference between

measured gamma passing rate with Delta ^{4}+ and Mobius Adapt 3%/3 mm, when Delta ^{4}+ geometrical uncertainty was taken into account. These results indicate 3%/3 mm criteria as the most appropriate for clinical use, since it is comparable to Delta ^{4}+ measurements. However, additional measurements can be performed where plans with incorporated known errors can be used to investigate the sensitivity of the independent dose calculation software. Therefore, it is advisable for the clinics to perform additional plan verification with Delta ^{4}+ phantom for a more complex treatment plans that have both high number of MU/Gy and larger treating sites.

Part VI

Conclusion

The results of the study show that online adaptation with Ethos for bladder cancer patients decrease CTV-PTV margins based on patients inter-fractional bladder variations. For the studied patients margins decreased by 13%- 59%. Absorbed dose to OAR in oART was PTV dependent, but generally improved for most patients compared to corresponding conventional IGRT plans. A statistical significant improvement in homogeneity was observed in adapted plans compared to scheduled. However, adaptive CI were still higher than IGRT due to on-couch and off-couch algorithms performance.

An independent dose calculation software Mobius Adapt was used for verification of adaptive sessions and validated with Delta^4+ phantom-based measurements.

To conclude, there are evident benefits of oART used for bladder cancer patient because it provides reduction of CTV-PTV margins, lower doses to healthy tissues while enabling target coverage.

References

[1] World Health Organisation. Global cancer observatory: cancer today, 2018. Available from: https://gco.iarc.fr/today.

[2] Kamat A, Let's Keep the Momentum Going, Urotoday, 2019. Availible from:https://www.urotoday.com/center-of-excellence/bladder-cancer.html

[3] Kibrom A.Z, Knight K.A. Adaptive radiation therapy for bladder cancer: a review of adaptive techniques used in clinical practice. J Med Radiat Sci. 2015;62(4):277–285. 10.1002/jmrs.129

[4] Podgorsak E.B. Radiation physics for medical physicists. International Atomic Energy Agency; 2016. p.606-640

[5] Burnet N.G, Thomas S.J, Burton K.E, Jefferies S.J. Defining the tumour and target volumes for radiotherapy. Cancer Imaging. 2004;4:153

[6] Grønborg C, Vestergaard A,Høyer M, Söhn M, Pedersen E.M, Petersen J.B, Agerbæk M, Muren L.P. Intra-fractional bladder motion and margins in adaptive radiotherapy for urinary bladder cancer, Acta Oncologica,2015:54:9, 1461-1466. 10.3109/0284186X.2015.1062138

[7] Viswanathan A.N, Yorke E.D, Marks L.B, Eifel P.J, Shipley W.U. Radiation dose-volume effects of the urinary bladder. Int. J. Radiat. Oncol. Biol. Phys. 2010;76:S116–S122. 10.1016/j.ijrobp.2009.02.090

[8] Berthelsen A.K, Dobbs J, Kjellen E, et al. What's new in target volume definition for radiologists in ICRU report 71 ? How can the ICRU volume definitions be integrated in clinical practice ? Cancer Imaging. 2007;7:104–116. 10.1102/1470-7330.2007.0013

[9] Jadon R, Higgins E, Hanna L, Evans M, Colen B, Staffurth J. A systematic review of dose-volume predictors and constraints for late bowel toxicity following pelvic radiotherapy. Radiat Oncol 14, 57 (2019). 10.1186/s13014-019-1262-8

[10] Michalski J.M, Gay H, Jackson A, Tucker SL, Deasy J.O. Radiation dose-volume effects in radiation-induced rectal injury [published correction appears in Int J Radiat Oncol Biol Phys. 2019 Aug 1;104(5):1185]. Int J Radiat Oncol Biol Phys. 2010;76(3 Suppl):S123-S129. 10.1016/j.ijrobp.2009.03.078

[11] Michalecki L, Gabryś D, Kulik R, Wydmański J, Trela K. Radiotherapy induced hip joint avascular necrosis-Two cases report. Rep Pract Oncol Radiother. 2011;16(5):198-201. Published 2011 May. 31.10.1016/j.rpor.2011.04.004

[12] Rana S. Intensity modulated radiation therapy versus volumetric intensity modulated arc therapy. J Med Radiat Sci. 2013;60:81–83. 10.1002/jmrs.19

[13] Prescribing, recording and reporting photon beam therapy (supplement to ICRU Report 50) (1999) Anonymous. Report 62, International Commission on Radiation Units and Measurements, Washington, DC.

[14] Varian Medical Systems. Ethos™ therapy AI: Technical Brief;2020.

[15] Bedford JL, Lee YK, Wai P, South CP, Warrington AP. Evaluation of the delta 4 phantom for IMRT and VMAT verification. Phys Med Biol. 2009;54: N167–N176. 10.1088/0031-9155/54/9/N04.

[16] Low D, Harms W, Mutic S,Purdy J. A technique for the quantitative evaluation of dose distributions. Med Phys . 1998 May;25(5):656-61. 10.1118/1.598248.

[17] Steers J.M, Fraass B.A. IMRT QA: Selecting gamma criteria based on error detection sensitivity. Med Phys. 2016;43:1982–94. 10.1118/1.4943953

[18] Yu L, Tang T.L.S, Cassim N, Livingstone A, Cassidy D , Kairn T, Crowe S.B. Analysis of dose comparison techniques for patient-specific quality assurance in radiation therapy. Journal of Applied Clinical Medical Physics. 2019 Nov;20(11):189-198. 10.1002/acm2.12726.

[19] Ozturk N, Smith B, Aydogan.SU-E-T-442: Comparison of Global versus Local Gamma Criteria for Planar Dose IMRT QA.Med. Phys. 38, 3590 (2011). 10.1118/1.3612396

[20] Nelms B.E, Simon J.A. A survey on IMRT QA analysis. J App Clin Med Phys. 2007;8(3):76–90

[21] Abolaban F, Zaman S, Cashmore J, Nisbet A, Clark C.H. Changes in patterns of intensity-modulated radiotherapy verification and quality assurance in the UK. Clin Oncol. 2016;28(8):e28–e34

[22] Ezzell G.A, Burmeister J.W, Dogan N, LoSasso T.J, Mechalakos J.G, Mihailidis D, Molineu A, Palta J.R, Ramsey C.R, Salter B.J. IMRT commissioning: Multiple institution planning and dosimetry comparisons, a report from AAPM Task Group 119. Med. Phys. 36, 5359– 5373 (2009). 10.1118/1.3238104

[23] Wu S, Chen J, Li Z, Qui Q, Wang X, Li C, Yin Y. Analysis of dose verification results for 924 intensity-modulated radiation therapy plans. Precision Radiation Oncology (2018). 10.1002/pro6.58

[24] Rajasekaran D, Jeevanandam P, Sukumar P, Ranganathan A, Johnjothi J, Nagarajan V. A study on the correlation between plan complexity and gamma index analysis in patient specific quality assurance of volumetric modulated arc therapy Rep Pract Oncol Radiother, 20 (2015), pp. 57-65. 0. 1016/j.rpor.2014.08.006

[25] Petrova D, Smickovska S, Lazarevska E. Conformity Index and Homogeneity Index of the Postoperative Whole Breast Radiotherapy. J Med Sci. 2017;5(6):736–739. 10.3889/oamjms.2017.161

[26] International Commission on Radiation Units and Measurements, Prescribing, Recording, and Reporting Photon-Beam Intensity-Modulated Radiation Therapy (IMRT). ICRU Report 83 2010.10.1093/jicru/ndq001

[27] Sadagopan R, Bencomo JA, Martin RL, Nilsson G, Matzen T, Balter PA. Characterization and clinical evaluation of a novel IMRT quality assurance system. J Appl Clin Med Phys. 2009;10(2):2928. Published 2009 May. 7.10.1120/jacmp.v10i2.2928

[28] Kang I.L, Koval J.J. Determination of the best significance level in forward stepwise logistic regression, Communications in Statistics - Simulation and Computation, 26:2, 559-575. 10.1080/03610919708813397

[29] Hubert M, Vandervieren E. An adjusted boxplot for skewed distributions Computational Statistics Data Analysis, 52 (12) (2008), pp. 5186-5201. 10.1016/j.csda.2007.11.008

[30] Viswanathan AN, Yorke ED, Marks LB, Eifel PJ, Shipley WU. Radiation dose-volume effects of the urinary bladder. Int J Radiat Oncol Biol Phys. 2010;76(3 Suppl):S116-S122. 10.1016/j.ijrobp.2009.02.090

Part VII

Appendix

A Volumetric and Dosimetric Data

Table 8: *CTV volume variations for adaptive sessions median values (Q_2), first quartile (Q_1), third quartile (Q_3) and interquartile ranges (IQR).*

	Q_2	Q_1	Q_3	IQR
Patient 1	265.8	249.4	326.0	77.3
Patient 2	70.6	68.6	78.0	9.4
Patient 3	155.3	144.5	213.6	69.1
Patient 4	152.6	138.2	155.8	17.6
Patient 5	99.05	79.2	108.0	28.9
Patient 6	269.9	239.6	299.7	60.1

Table 9: *Achieved PTV coverage median values (Q_2), first quartile (Q_1), third quartile (Q_3) and interquartile ranges (IQR) for adapted (to the left) and scheduled plans (to the right).*

Adapted	Q_2	Q_1	Q_3	IQR
Patient 1	99.8	99.8	99.8	0.0
Patient 2	100.0	100.0	100	0.0
Patient 3	99.9	99.9	100	0.1
Patient 4	100.0	99.6	100	0.4
Patient 5	100.0	99.9	100	0.1
Patient 6	99.9	99.9	100	0.1

Scheduled	Q_2	Q_1	Q_3	IQR
Patient 1	92.6	84.1	94.7	10.6
Patient 2	98.0	95.8	99.2	3.4
Patient 3	99.7	93.8	99.9	6.2
Patient 4	90.8	88.2	94.6	6.4
Patient 5	93.8	91.5	96.7	5.2
Patient 6	79.7	71.2	82.5	11.3

Table 10: *Achieved obowel bag V_{45Gy} median values (Q_2), first quartile (Q_1), third quartile (Q_3) and interquartile ranges (IQR) for adapted (to the left) and scheduled plans (to the right).*

Adapted	Q_2	Q_1	Q_3	IQR
Patient 1	333.1	316.9	348.9	32
Patient 2	26.5	24.4	32	7.6
Patient 3	366.2	346.9	372.5	25.5
Patient 4	281.7	271.7	286.5	14.8
Patient 5	116.6	103.2	128.0	24.8
Patient 6	187.7	172.4	197.2	24.8

Scheduled	Q_2	Q_1	Q_3	IQR
Patient 1	327.2	295.1	354.3	59.2
Patient 2	23.0	20.3	32.2	11.9
Patient 3	380.8	343.3	387.8	44.6
Patient 4	243.9	241.5	249.5	8.0
Patient 5	145.2	132.4	152.7	20.4
Patient 6	132.9	120.9	144.35	23.4

Table 11: *Achieved obowel bag V_{30Gy} median values (Q_2), first quartile (Q_1), third quartile (Q_3) and interquartile ranges (IQR) for adapted (to the left) and scheduled plans (to the right).*

Adapted	Q_2	Q_1	Q_3	IQR
Patient 1	433.9	415	457	42
Patient 2	61.4	58.5	66.4	7.9
Patient 3	570.4	566.3	611.5	45.3
Patient 4	396.1	388.7	402.8	14.1
Patient 5	186.6	166,1	195.9	29.8
Patient 6	382.2	272.4	348.8	76.4

Scheduled	Q_2	Q_1	Q_3	IQR
Patient 1	418.5	390	354.3	62.6
Patient 2	57.0	52.7	71.8	19.1
Patient 3	577.0	539.3	592.05	52.8
Patient 4	335.8	328.2	342.3	14.1
Patient 5	233.6	217.4	252.9	29.8
Patient 6	252.8	238.1	276.1	38

Table 12: *Achieved rectum V_{50Gy} median values (Q_2), first quartile (Q_1), third quartile (Q_3) and interquartile ranges (IQR) for adapted (to the left) and scheduled plans (to the right).*

Adapted	Q_2	Q_1	Q_3	IQR
Patient 1	16.9	16.2	18.2	2
Patient 2	0.0	0.0	0.0	0.0
Patient 3	0.4	0.2	0.7	0.5
Patient 4	11.0	9.6	12.6	3.0
Patient 5	7.8	5.7	9.3	3.7
Patient 6	0.7	0.0	1.2	1.2

Scheduled	Q_2	Q_1	Q_3	IQR
Patient 1	14.5	12.7	18.6	5.9
Patient 2	0.0	0.0	0.0	0.0
Patient 3	1.2	0.6	3.1	2.6
Patient 4	15.2	13.2	18.7	5.4
Patient 5	8.1	5.3	12.3	7.3
Patient 6	0.0	0.0	0.0	0.0

Table 13: *Achieved rectum V_{40Gy} median values (Q_2), first quartile (Q_1), third quartile (Q_3) and interquartile ranges (IQR) for adapted (to the left) and scheduled plans (to the right).*

Adapted	Q_2	Q_1	Q_3	IQR
Patient 1	29.6	27.4	30.5	3.1
Patient 2	2.5	1.1	4.6	3.5
Patient 3	19.4	14.7	24.6	9.9
Patient 4	26.4	25.3	32.3	7.0
Patient 5	19.3	15.7	20.4	4.8
Patient 6	6.8	5.4	9.2	3.8

Scheduled	Q_2	Q_1	Q_3	IQR
Patient 1	26.7	21.4	27.8	6.4
Patient 2	3.4	2.3	6.2	3.4
Patient 3	22.3	19.2	26.3	7.2
Patient 4	38.5	34.2	48.9	14.7
Patient 5	19.8	15.6	24.3	8.7
Patient 6	0.0	238.1	0.1	0.1

B Correlation Figures

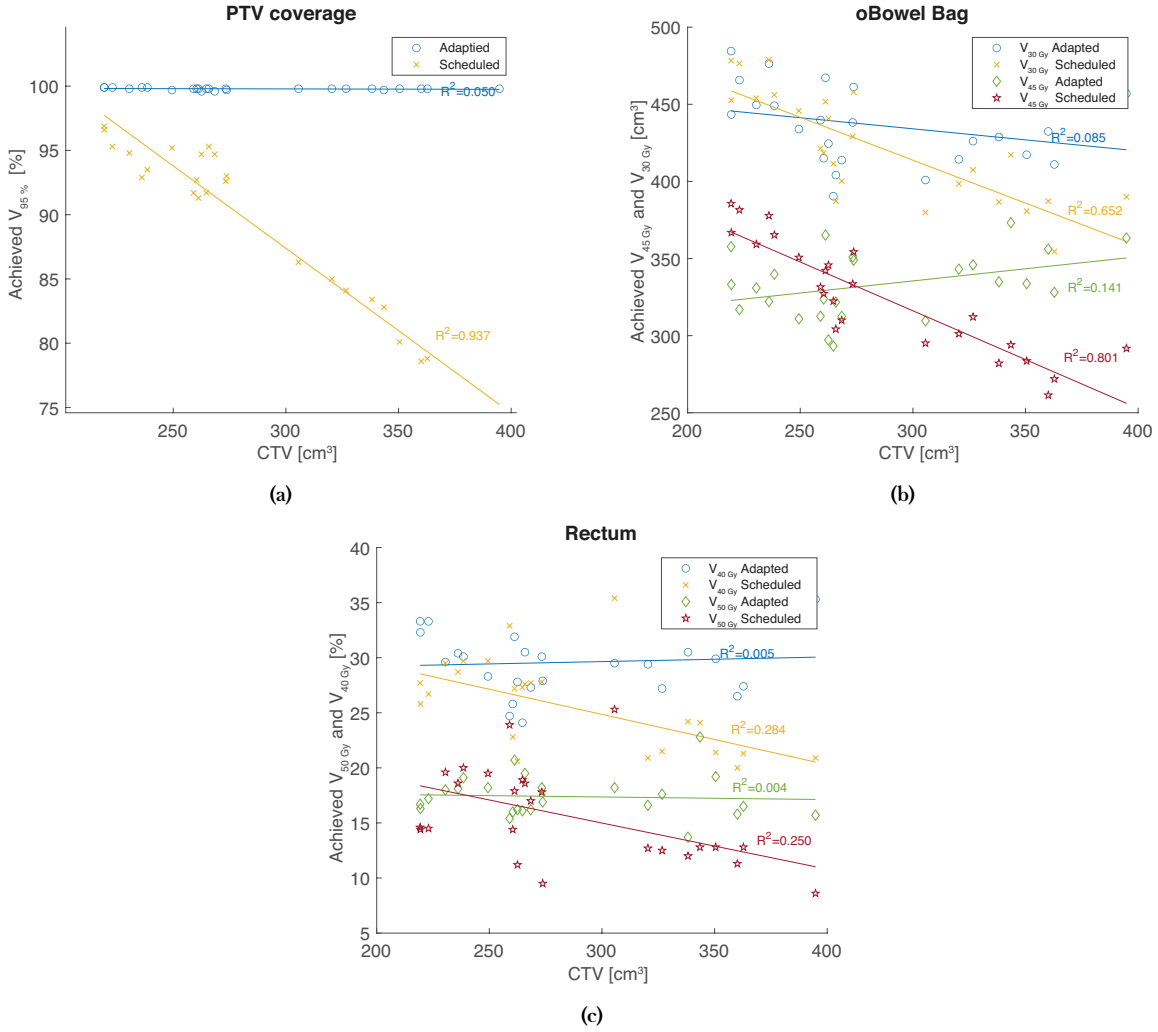

Figure 18: *Correlation plots for bladder volume variations VS absorbed dose to OAR for different clinical constraints for scheduled and adapted plans for Patient 1. Top left corner PTV coverage 18a, top right corner obowel bag 18b and at the bottom rectum 18c.*

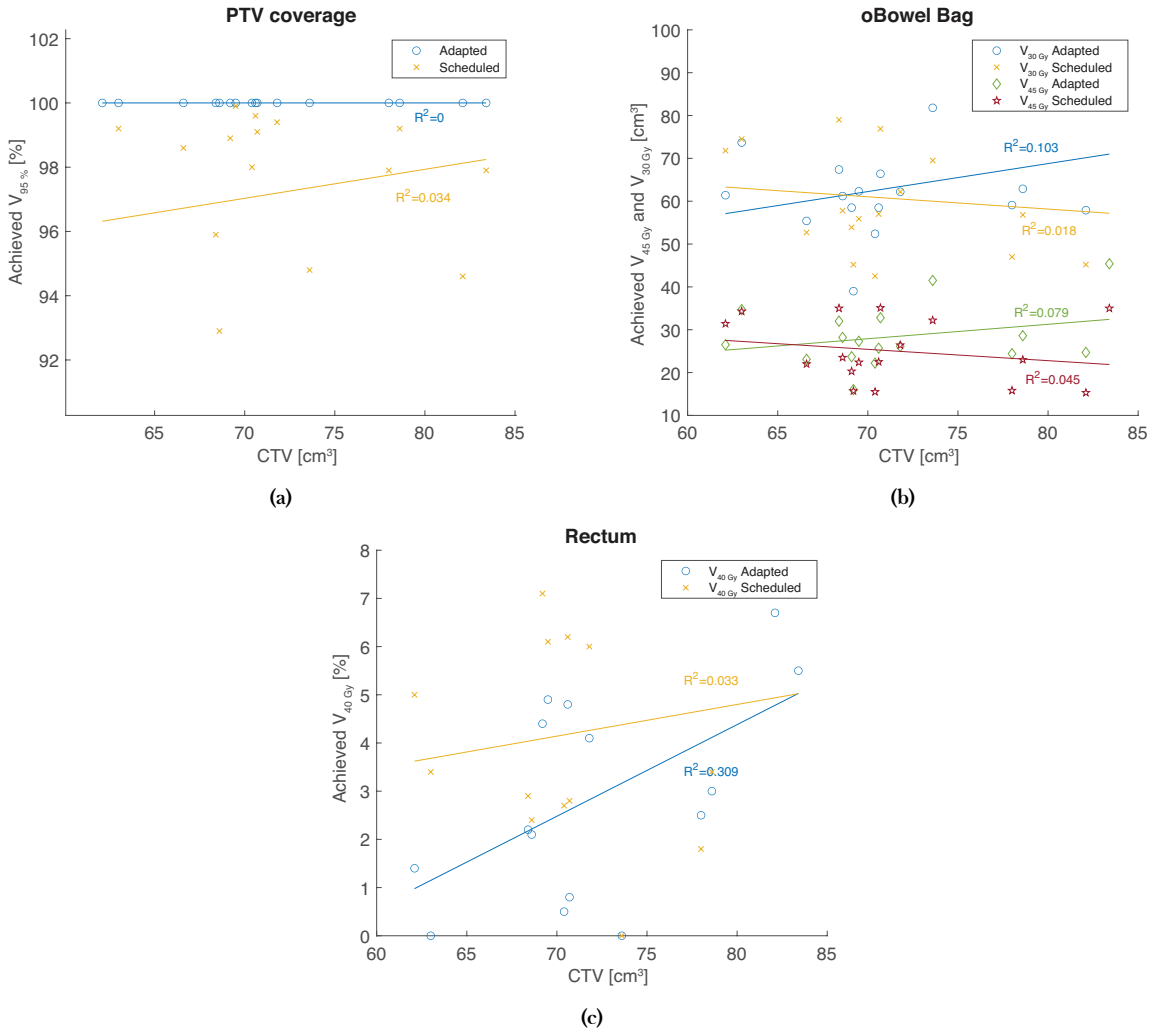

Figure 19: *Correlation plots for bladder volume variations VS absorbed dose to OAR for different clinical constraints for scheduled and adapted plans for Patient 2. Top left corner PTV coverage 19a, top right corner obowel bag 19b and at the bottom rectum 19c.*

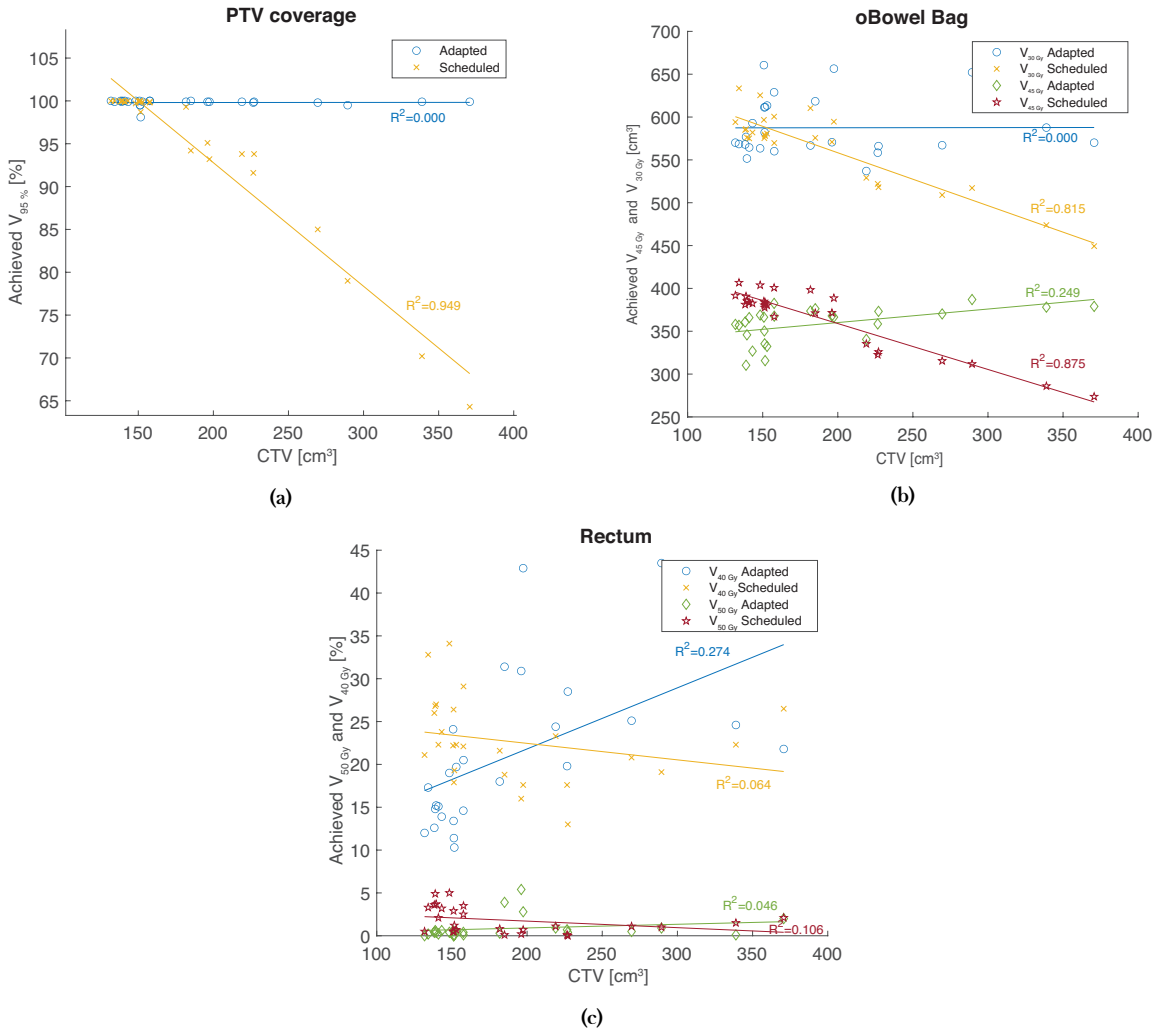

Figure 20: *Correlation plots for bladder volume variations VS absorbed dose to OAR for different clinical constraints for scheduled and adapted plans for Patient 3. Top left corner PTV coverage 20a, top right corner obowel bag 20b and at the bottom rectum 20c.*

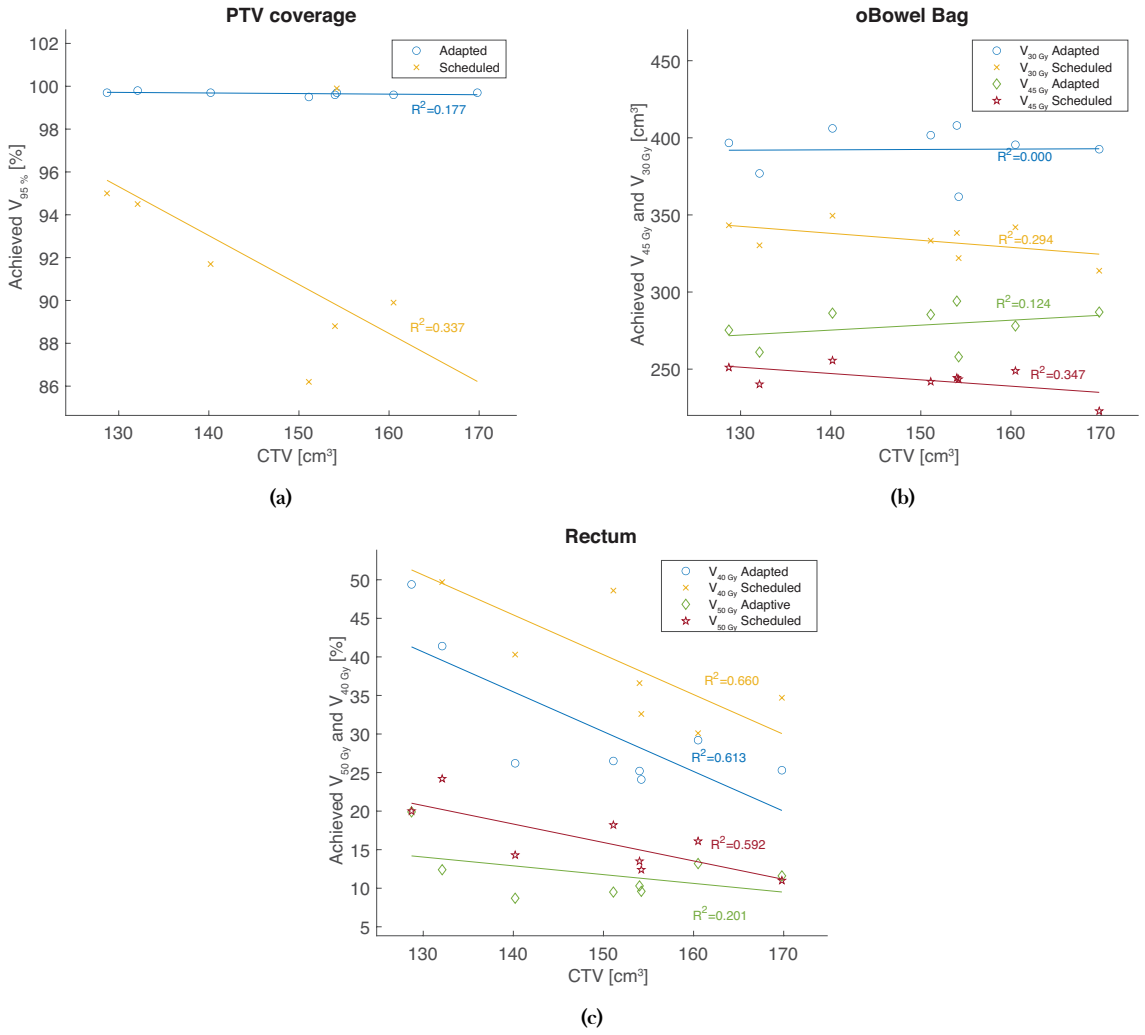

Figure 21: *Correlation plots for bladder volume variations VS absorbed dose to OAR for different clinical constraints for scheduled and adapted plans for Patient 4. Top left corner PTV coverage 21a, top right corner obowel bag 21b and at the bottom rectum 21c.*

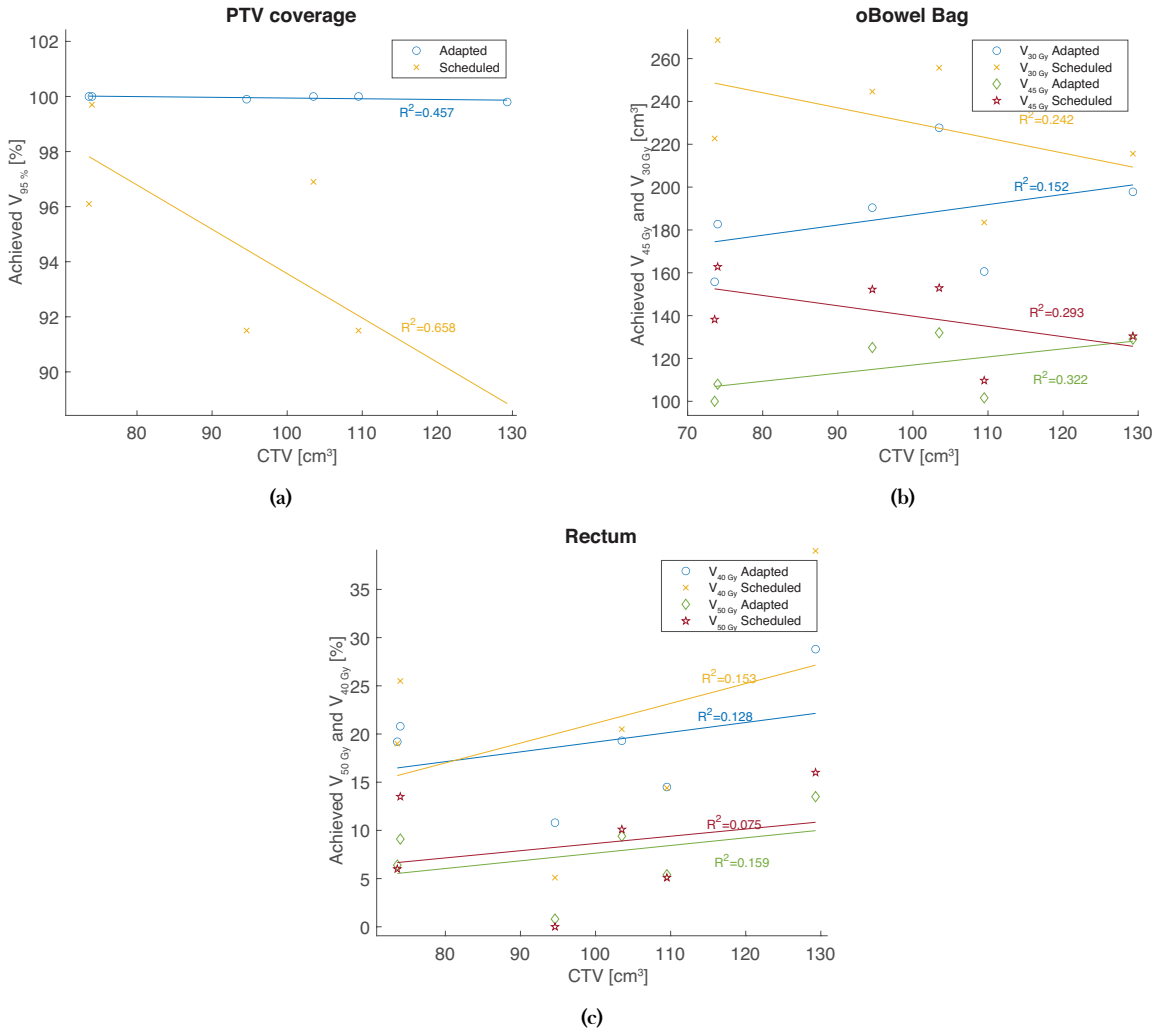

Figure 22: *Correlation plots for bladder volume variations VS absorbed dose to OAR for different clinical constraints for scheduled and adapted plans for Patient 5. Top left corner PTV coverage 22a, top right corner obowel bag 22b and at the bottom rectum 22c*

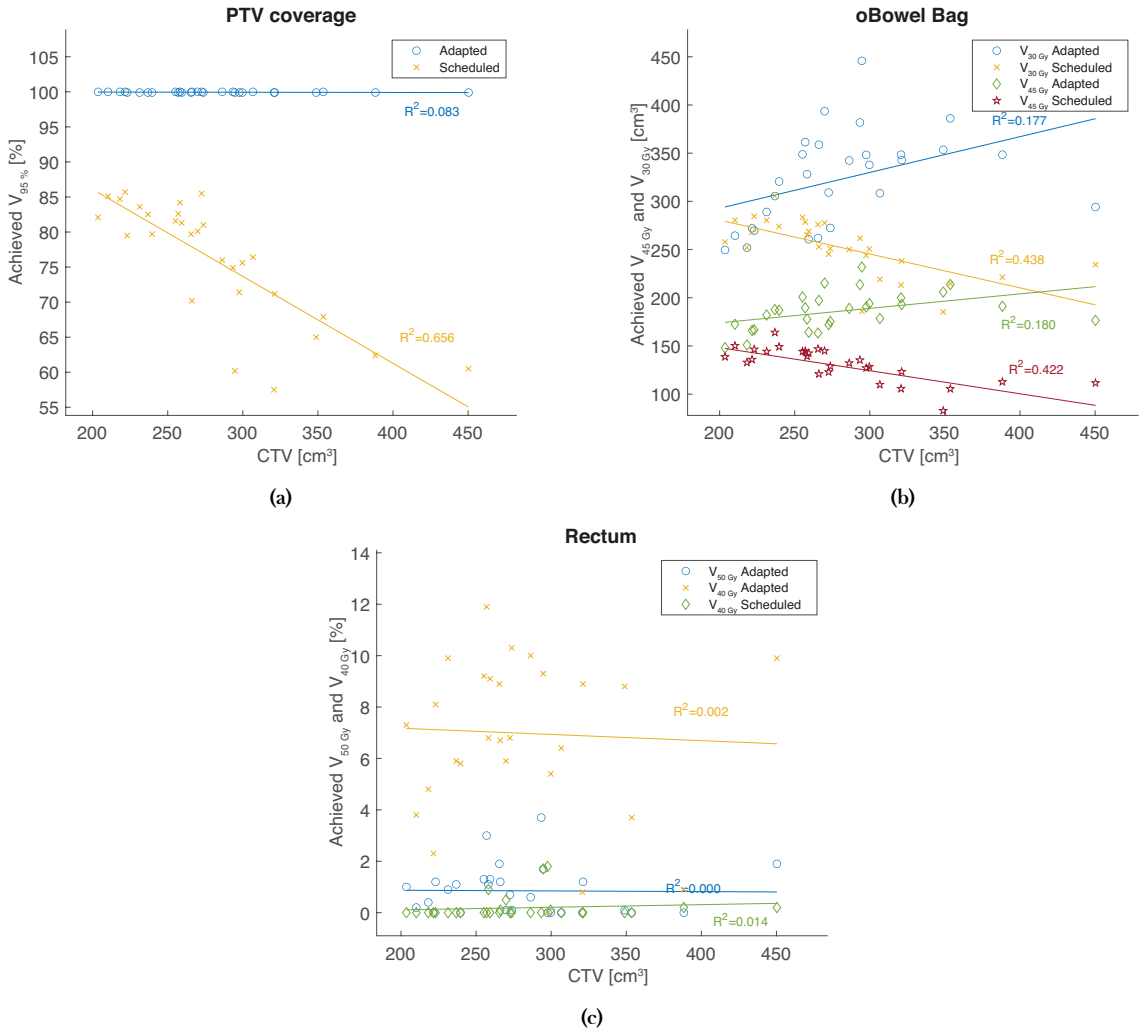

Figure 23: *Correlation plots for bladder volume variations VS absorbed dose to OAR for different clinical constraints for scheduled and adapted plans for Patient 6. Top left corner PTV coverage 23a, top right corner obowel bag 23b and at the bottom rectum 23c.*

C CI and HI Data

Table 14: *Calculated CI median values (Q_2), first quartile (Q_1), third quartile (Q_3) and interquartile ranges (IQR) for adapted (to the left) and scheduled plans (to the right).*

Adapted	Q_2	Q_1	Q_3	IQR
Patient 1	1.08	1.08	1.09	0.013
Patient 2	1.25	1.24	1.26	0.016
Patient 3	1.09	1.08	1.11	0.025
Patient 4	1.08	1.08	1.09	0.018
Patient 5	1.16	1.15	1.19	0.030
Patient 6	1.16	1.15	1.18	0.032

Scheduled	Q_2	Q_1	Q_3	IQR
Patient 1	1.04	1.00	1.18	0.013
Patient 2	1.23	1.15	1.27	0.016
Patient 3	1.35	1.05	1.45	0.025
Patient 4	1.00	0.97	1.06	0.018
Patient 5	1.31	1.27	1.48	0.030
Patient 6	0.83	0.72	0.91	0.032

Table 15: *Calculated HI median values (Q_2), first quartile (Q_1), third quartile (Q_3) and interquartile ranges (IQR) for adapted (to the left) and scheduled plans (to the right).*

Adapted	Q_2	Q_1	Q_3	IQR
Patient 1	0.050	0.048	0.051	0.003
Patient 2	0.025	0.023	0.027	0.004
Patient 3	0.049	0.047	0.058	0.157
Patient 4	0.061	1.08	1.09	0.017
Patient 5	0.034	0.029	0.034	0.005
Patient 6	0.032	0.030	0.036	0.006

Scheduled	Q_2	Q_1	Q_3	IQR
Patient 1	0.022	0.020	0.024	0.004
Patient 2	0.075	0.053	0.131	0.078
Patient 3	0.068	1.05	0.058	0.094
Patient 4	0.19	0.971	1.06	0.085
Patient 5	0.26	0.137	0.334	0.19
Patient 6	0.44	0.357	0.715	0.34

D PSQA Data

Table 16: *Median (Q_2), first quartile (Q_1), third quartile (Q_3) and and interquartile ranges (IQR) for Delta^4+ phantom measurements and Mobius Adapt different criteria for patient 1*

Patient 1				
	Q_2	Q_1	Q_3	IQR
Delta^4+ 3%/2mm	84.8	84.0	93.7	9.8
Mobius 3D 3%/3mm	99.7	99.7	99.8	0.1
Mobius 3D 3%/2mm	99.5	99.3	99.5	0.2
Mobius 3D 2%/2mm	96.1	95.8	96.4	0.6

Table 17: *Median (Q_2), first quartile (Q_1), third quartile (Q_3) and and interquartile ranges (IQR) for Delta^4+ phantom measurements and Mobius Adapt different criteria for patient 2*

Patient 2				
	Q_2	Q_1	Q_3	IQR
Delta^4+ 3%/2mm	99.8	99.8	100	0.2
Mobius 3D 3%/3mm	99.9	99.7	100	0.3
Mobius 3D 3%/2mm	99.5	99.3	99.6	0.3
Mobius 3D 2%/2mm	97.5	97.3	97.9	0.6

Table 18: *Median (Q_2), first quartile (Q_1), third quartile (Q_3) and and interquartile ranges (IQR) for Delta^4+ phantom measurements and Mobius Adapt different criteria for patient 3*

Patient 3				
	Q_2	Q_1	Q_3	IQR
Delta^4+ 3%/2mm	94.3	93.2	95.7	2.5
Mobius 3D 3%/3mm	99.8	99.7	99.9	0.2
Mobius 3D 3%/2mm	99.4	99.4	99.6	0.2
Mobius 3D 2%/2mm	97.8	97.7	98.0	0.3
45° Delta^4 3%/3mm	99.8	99.6	100.0	0.4

Table 19: *Median (Q_2), first quartile (Q_1), third quartile (Q_3) and and interquartile ranges (IQR) for Delta^4+ phantom measurements and Mobius Adapt different criteria for patient 4*

Patient 4				
	Q_2	Q_1	Q_3	IQR
Delta^4+ 3%/2mm	92.7	91.6	93.4	2.15
Mobius 3D 3%/3mm	99.7	99.7	99.8	0.1
Mobius 3D 3%/2mm	99.2	99.0	99.5	0.5
Mobius 3D 2%/2mm	96.6	96.1	97.2	1.1

Table 20: *Median (Q_2), first quartile (Q_1), third quartile (Q_3) and and interquartile ranges (IQR) for Delta^4+ phantom measurements and Mobius Adapt different criteria for patient 5*

Patient 5				
	Q_2	Q_1	Q_3	IQR
Delta^4+ 3%/2mm	98.4	98.2	98.7	0.5
Mobius 3D 3%/3mm	99.8	99.8	99.9	0.1
Mobius 3D 3%/2mm	99.6	99.5	99.7	0.2
Mobius 3D 2%/2mm	99.6	99.5	99.7	0.2

Table 21: *Median (Q_2), first quartile (Q_1), third quartile (Q_3) and and interquartile ranges (IQR) for Delta^4 + phantom measurements and Mobius Adapt different criteria for patient 6*

Patient 6				
	Q_2	Q_1	Q_3	IQR
Delta^4+ 3%/2mm	84.8	84.0	93.8	9.8
Mobius 3D 3%/3mm	99.7	99.7	99.8	0.1
Mobius 3D 3%/2mm	99.4	99.3	99.5	0.2
Mobius 3D 2%/2mm	96.1	95.8	96.4	0.6
45° Delta^4+ 3%/3mm	99.5	99.3	99.6	0.3